Computer Methods in Applied Mechanics and Engineering 199 (2010) 2472–2486

Contents lists available at ScienceDirect

Computer Methods in Applied Mechanics and Engineering

journal homepage: www.elsevier.com/locate/cma

Solution verification, goal-oriented adaptive methods for stochastic advection–diffusion problems

Regina C. Almeida [a,b], J. Tinsley Oden [b,*]

[a] Department of Computational Mechanics, Laboratório Nacional de Computação Científica/MCT, Brazil
[b] Institute for Computational Engineering and Sciences, The University of Texas at Austin, USA

ARTICLE INFO

Article history:
Received 16 October 2009
Received in revised form 8 April 2010
Accepted 10 April 2010
Available online 21 April 2010

Keywords:
Goal-oriented adaptivity
Stochastic advection–diffusion equations
Stochastic collocation method

ABSTRACT

A goal-oriented analysis of linear, stochastic advection–diffusion models is presented which provides both a method for solution verification as well as a basis for improving results through adaptation of both the mesh and the way random variables are approximated. A class of model problems with random coefficients and source terms is cast in a variational setting. Specific quantities of interest are specified which are also random variables. A stochastic adjoint problem associated with the quantities of interest is formulated and a posteriori error estimates are derived. These are used to guide an adaptive algorithm which adjusts the sparse probabilistic grid so as to control the approximation error. Numerical examples are given to demonstrate the methodology for a specific model problem.

1. Introduction

The idea of solution verification concerns the processes of determining if results produced by a numerical approximation of a mathematical model represent the exact solutions with sufficient accuracy. It is generally accepted that this question can only be addressed through a posteriori error estimation. For deterministic systems, the use of so-called goal-oriented methods has provided an approach to develop a posteriori estimates of specific quantities of interest and to, therefore, provide solution verification for specific target outputs. In the present work we develop goal-oriented approaches for a class of stochastic partial differential equations governing transport phenomena: the linear advection–diffusion problem.

The conception of goal-oriented methods for the numerical solution of partial differential equations was introduced in [1,2] as a family of computational procedures aimed at accomplishing the principal mission of computer modeling and simulation: the calculation of specific quantities of interest, or target outputs. While error estimation and control in traditional finite element schemes, for example, deal with global features of solutions, such as total energy (e.g. [1,2]), goal-oriented methods are designed to control approximation error in local features of the solution, generally defined by linear functionals on the trial space containing the solution. Over the last decade, goal-oriented methods have been developed for estimating and controlling approximation error in a broad class of models characterized by deterministic partial differential equations (see [1–6]). More recently, goal-oriented methods have been extended to techniques for controlling relative modeling error and have been used in adaptive modeling algorithms (see, e.g. [5–7]).

In the present investigation, we consider extensions of the theory of goal-oriented methods to a model class of stochastic partial differential equations describing the transport of a scalar-valued species concentration in time over a fixed spatial domain. Of specific interest are cases in which the model parameters (velocity field and diffusivity coefficient) and the sources are random fields. The general approach involves the calculation of adjoints and residuals, as in the deterministic case, but here the added complications of solving the stochastic forward problem and backward problem arises.

The numerical solution of stochastic partial differential equations has undergone significant development in the last two decades and several new approaches have been contributed. These include spectral methods [8], Galerkin finite element methods [9–12] (so-called stochastic Galerkin or stochastic finite element methods), stochastic collocation methods [13–16] and stochastic fast multipole methods [17]. References to additional works can be found in [8,18]. A common aspect of many of these studies is to lay down assumptions on the random coefficients that makes possible the introduction of a finite (truncated) Karhunen–Loève approximation of random fields, which reduces the dependence of the random features of the solution to a finite number of random vectors. Furthermore, these vectors can be mapped into bounded intervals of $\mathbb{R}$, which reduces the analysis to essentially a large deterministic system. We adopt a similar approach in the present study.

Following this introduction, we review the structure of the deterministic forward problem and its adjoint for specific quantities of interest. We then extend the formulation to stochastic systems in which the velocity field, the diffusion coefficient and the source terms

* Corresponding author.
E-mail addresses: rcca@lncc.br (R.C. Almeida), oden@ices.utexas.edu (J.T. Oden).

0045-7825/$ – see front matter © 2010 Elsevier B.V. All rights reserved.
doi:10.1016/j.cma.2010.04.001

are random variables. We invoke several assumptions concerning the random parameters and sources which render them representable by a truncated Karhunen–Loève expansion, which we demonstrate allows the forward and adjoint problems to be reformulated in terms of a joint probability density ρ and N real random variables representing the maps of N random vectors appearing in the Karhunen–Loève expansion. We go on to develop finite element and stochastic collocation approximations of the stochastic system and then a posteriori estimates of errors in the quantities of interest. These allow one to develop adaptive algorithms that control mesh size, polynomial interpolation order and even the number of terms in the Karhunen–Loève expansion so as to meet preset tolerances in errors in quantities of interest. The results of preliminary experiments on model problems are given.

2. Linear advection–diffusion in a deterministic setting

A class of physical phenomena encountered in many important applications, ranging from environmental remediation, dispersion of toxic substances, or transport of biological species in the atmosphere, involves the transport of a species in time through diffusion and advection over a spatial domain. One is interested in the concentration of that species over specific time intervals at specific locations in the domain. Understandably, there may be significant uncertainties in physical parameters and in environmental conditions involved in such events. One of the simplest models that captures the essential features is that of linear, time-dependent advection–diffusion process.

The classical deterministic model of the transport of a species with concentration $u(\boldsymbol{x},t)$ at a point $\boldsymbol{x}$ and time t through an open bounded domain $D\subset\mathbb{R}^d$ with Lipschitz boundary ∂D is characterized by the initial boundary-value problem of finding u such that

$$\begin{array}{lll} Au(\boldsymbol{x},t)=f & \text{at} & (\boldsymbol{x},t)\in D\times(0,T);\\ Bu(\boldsymbol{x},t)=g & \text{at} & (\boldsymbol{x},t)\in\Gamma_N\times(0,T);\\ u=0 & \text{at} & (\boldsymbol{x},t)\in\Gamma_D\times(0,T);\\ u(0)=u_0 & \text{at} & \boldsymbol{x}\in\overline{D},t=0, \end{array} \tag{1}$$

where Γ_D and Γ_N denote portions of the boundary such that $\overline{\Gamma}_D\cup\overline{\Gamma}_N=\partial D$, $\overline{\Gamma}_D\cap\overline{\Gamma}_N=\emptyset$, and

$$\begin{array}{l} Au=\partial_t u+\boldsymbol{w}\cdot\nabla u-\nabla\cdot\mathcal{K}\nabla u;\\ Bu=\boldsymbol{n}\cdot\mathcal{K}\nabla u;\\ u(0)=u(\boldsymbol{x},0),\boldsymbol{x}\in\overline{D}. \end{array} \tag{2}$$

Here, $\partial_t(\cdot)=\partial(\cdot)/\partial t$, ∇ is the gradient with respect to $\boldsymbol{x}$, $f=f(\boldsymbol{x},t)$ is the given source intensity, $\mathcal{K}=\mathcal{K}(\boldsymbol{x})$ a diffusion modulus, $\boldsymbol{w}=\boldsymbol{w}(\boldsymbol{x},t)$ a prescribed velocity field over D, g a prescribed flux, $\boldsymbol{n}$ is a unit exterior normal vector on ∂D, and $u_0=u_0(\boldsymbol{x})$ is the initial data.

To cast Eq. (1) in a weak or function-space setting, we introduce the spaces:

$$\begin{array}{l} Z=\left\{z\in H^1(\Omega);z=0\ on\ \Gamma_D\right\};\\ V=\left\{v\in L^2(0,T;Z);\partial_t v\in L^2(0,T;Z')\right\}, \end{array}$$

where Z' is the dual space of Z. Consider the following bilinear form:

$$\begin{array}{lcl} a(\cdot,\cdot) & : & V\times V\to\mathbb{R};\\ a(z,v) & = & \displaystyle\int_0^T\int_D[\partial_t zv+\boldsymbol{w}\cdot\nabla zv+\mathcal{K}\nabla z\cdot\nabla v]d\boldsymbol{x}dt+\int_D z(0)v(0)d\boldsymbol{x}. \end{array} \tag{3}$$

A formal integration by parts of the diffusive term, assuming for the moment that the integrand functions are smooth enough, yields

$$a(z,v)=\int_0^T\int_D(Az)v\,d\boldsymbol{x}dt+\int_0^T\int_{\Gamma_N}(Bz)v\,dsdt+\int_D z(0)v(0)d\boldsymbol{x} \tag{4}$$

and, with a further integration,

$$a(z,v)=\int_0^T\int_D(A^*v)z\,d\boldsymbol{x}dt+\int_0^T\int_{\Gamma_N}(B^*v)z\,dsdt+\int_D v(T)z(T)d\boldsymbol{x}, \tag{5}$$

where the adjoints (A^*, B^*) are given by

$$\begin{array}{l} A^*v=-\partial_t v-\boldsymbol{w}\cdot\nabla v-(\nabla\cdot\boldsymbol{w})v-\nabla\cdot\mathcal{K}\nabla v;\\ B^*v=-\boldsymbol{n}\cdot\mathcal{K}\nabla v+(\boldsymbol{n}\cdot\boldsymbol{w})v. \end{array} \tag{6}$$

It follows that if we set $z=u$ in Eq. (3), u being a solution of Eq. (1), then, $\forall v\in v$, the problem of finding u such that

$$a(u,v)=F(v)+\int_D u_0v(0)d\boldsymbol{x},\forall v\in V, \tag{7}$$

where

$$F(v)=\int_0^T\left(\int_D fv\,d\boldsymbol{x}+\int_{\Gamma_N}gv\,ds\right)dt, \tag{8}$$

is a weak statement of the advection–diffusion problem (1), in which the initial condition is weakly imposed.

Let $Q:V\to\mathbb{R}$ be a continuous linear functional on V. The functional Q will represent a quantity of interest: a target output representing a goal of the model defined in Eq. (1) (and Eq. (7)). An example of Q is

$$Q(v)=\frac{1}{|\boldsymbol{\omega}|}\int_0^T\int_{\omega}q(v)d\boldsymbol{x}dt,$$

where ω is a bounded set in D and $q:V\to L^1(0,T;\omega)$ is a bounded linear operator; for example $q(v)=v$ or $q(v)(\boldsymbol{x})=k_\epsilon(\boldsymbol{x},\boldsymbol{x}_0)v(\boldsymbol{x})$, $\boldsymbol{x}_0\in\boldsymbol{\omega}$, and k_ε is a smooth kernel function which vanishes for $|\boldsymbol{x}-\boldsymbol{x}_0|>\varepsilon$. The problem of finding $p\in V$ such that

$$a(v,p)=Q(v),\quad\forall v\in V, \tag{9}$$

is called the adjoint (or dual) problem for Eq. (7). Problem (7) is the forward advection–diffusion problem while Eq. (9) is the backward (in time) advection–diffusion problem. The solution p is the adjoint solution or generalized Green's function corresponding to the particular quantity of interest Q. Formally, Eq. (9) is equivalent to the adjoint problem

$$\begin{array}{lll} A^*p=q & \text{at} & (\boldsymbol{x},t)\in D\times(0,T);\\ B^*p=0 & \text{at} & (\boldsymbol{x},t)\in\Gamma_N\times(0,T);\\ p=0 & \text{at} & (\boldsymbol{x},t)\in\Gamma_D\times(0,T);\\ p(T)=0 & \text{at} & t=T. \end{array} \tag{10}$$

We observe that

$$\begin{array}{rl} Q(u) & =\displaystyle\int_0^T\int_D(A^*p)u\,d\boldsymbol{x}dt+\int_0^T\int_{\Gamma_N}(B^*p)u\,dsdt+\int_D p(T)u(T)d\boldsymbol{x}\\ & =\displaystyle\int_0^T\int_D[\partial_t up+\boldsymbol{w}\cdot\nabla u\ p+\mathcal{K}\nabla u\cdot\nabla p]d\boldsymbol{x}dt\\ & \quad+\displaystyle\int_D u(0)p(0)d\boldsymbol{x}-\int_D u_0p(0)d\boldsymbol{x}\\ & =F(p) \end{array} \tag{11}$$

which is the classical property of Green's function p corresponding to the quantity of interest Q. Note that the time-reversed adjoint

problem (10) is well-posed only if the initial condition at the final time T is given so that we set $p(T)=0$.

3. The stochastic advection–diffusion problem

In more realistic settings, the key parameters in models of advection–diffusion processes can possess uncertainties due to random variability or, in particular, due to our ignorance in their values. It is therefore natural to treat these features as random fields and the solutions of the forward and adjoint problems as random fields. To reformulate problems (7) (or Eq. (1)) and (9) (or Eq. (10)) in such a stochastic setting, we must introduce additional assumptions and definitions on the mathematical framework and spaces on which the stochastic weak forms of the forward and backward problems are constructed. Toward this end, we introduce the following notations, definitions, and conventions:

- $(\Omega,\mathcal{U},\mathbb{P})$ is a complete probability space, with Ω the set of outcomes θ, $\mathcal{U}$ is the σ-algebra of events, and $\mathbb{P}:\mathcal{U}\to[0,1]$ a probability measure;
- $\boldsymbol{w}:(\Omega\times D\times[0,\ T])\to\mathbb{R}^d$, $\mathcal{K}:(\Omega\times D)\to\mathbb{R}$, $f:(\Omega\times D\times[0,\ T])\to\mathbb{R}$, the random velocity field, diffusion coefficient and source, which are assumed to have continuous and bounded covariance functions, and $\boldsymbol{w}$, $\mathcal{K}$ and f are measurable with respect to $\mathcal{U}\otimes\mathcal{B}(D\times[0,T])$, $\mathcal{U}\otimes\mathcal{B}(D)$ and $\mathcal{U}\otimes\mathcal{B}(D\times[0,T])$, where $\mathcal{B}(D)$ (respectively $\mathcal{B}(D\times[0,T])$) are the Borel σ-algebras generated by open subsets of D (and $D\times[0,T]$);
- let $\boldsymbol{Y}:\Omega\to\mathbb{R}^N$ be an N-dimensional random variable in $(\Omega,\ U,\ \mathbb{P})$. Thus, for each Borel set $\mathbb{B}\in\mathcal{B}(\mathbb{R}^N)$ we have $\boldsymbol{Y}^{-1}(\mathbb{B})\in\mathcal{U}$ and the distribution measure for $\boldsymbol{Y}$ is given by

$$\mu_{\boldsymbol{Y}}(\mathbb{B})=\mathbb{P}\left(\boldsymbol{Y}^{-1}(\mathbb{B})\right); \tag{12}$$

- with $1\le q<\infty$, we define the space

$$\begin{aligned}\left(L^q_{\mathbb{P}}(\Omega)\right)^N \quad &= \quad \{\boldsymbol{Y}:\Omega\to\mathbb{R}^N\,|\,\boldsymbol{Y}\text{is a random vector in}\,(\Omega,\mathcal{U},\mathbb{P}) \\ &\text{such that}\sum_{i=1}^{N}\int_{\Omega}|Y_i(\theta)|^q d\mathbb{P}(\theta)<\infty\};\end{aligned} \tag{13}$$

- assuming $\mu_{\boldsymbol{Y}}$ to be absolutely continuous with respect to the Lebesgue measure $d\boldsymbol{y}$, which we assume hereafter to be the case, there exists a probability density function $\rho(\boldsymbol{y})$, $\boldsymbol{y}\in\mathbb{R}^N$, such that $\rho:\mathbb{R}^N\to[0,\infty)$ and $d\mu_{\boldsymbol{Y}}=\rho(\boldsymbol{y})d\boldsymbol{y}$. Then, for $\boldsymbol{Y}\in L^1_{\mathbb{P}}(\Omega)$, its expected value is

$$\mathbb{E}[\boldsymbol{Y}]=\int_{\Omega}\boldsymbol{Y}(\theta)d\mathbb{P}(\theta)=\int_{\mathbb{R}^N}\boldsymbol{y}\rho(\boldsymbol{y})d\boldsymbol{y}; \tag{14}$$

- for $\boldsymbol{Y}\in(L^q_{\mathbb{P}}(\Omega))^N$, there exists a positive–definite covariance matrix,

$$\mathbb{C}ov[\boldsymbol{Y}]\in\mathbb{R}^{N\times N}; \tag{15}$$

$$\mathbb{C}ov[\boldsymbol{Y}]_{ij}=\mathbb{E}\left[(Y_i-\mathbb{E}[Y_i])\left(Y_j-\mathbb{E}\left[Y_j\right]\right)\right],\quad i,j=1,\ldots,N. \tag{16}$$

For a real-value function $v:\Omega\times\mathbb{R}^d$, $v=v(\theta,\boldsymbol{x})$,

$$\mathbb{C}ov[v]\left(\boldsymbol{x},\boldsymbol{x}'\right)\overset{def}{=}\mathbb{C}ov\left(v(\cdot,\boldsymbol{x}),v\left(\cdot,\boldsymbol{x}'\right)\right); \tag{17}$$

- product Hilbert spaces can be introduced which connect the random variables to the functions defined on $D\times[0,\ T]$. For example, if we write

$$\begin{aligned}V&=L^2\left(0,T;H^1(D)\otimes L^2_{\mathbb{P}}(\Omega)\right),\\ U&=L^2\left(0,T;H^{-1}(D)\otimes L^2_{\mathbb{P}}(\Omega)\right),\end{aligned} \tag{18}$$

an inner product on V is given by

$$(v,z)_V=\int_0^T\int_D\int_{\Omega}\nabla z\cdot\nabla v\quad dxdtd\mathbb{P}(\theta), \tag{19}$$

where $v=v(\theta,\boldsymbol{x},t)$ and $z=z(\theta,\boldsymbol{x},t)$;

- to guarantee existence and uniqueness for the stochastic solution $u(\theta,\boldsymbol{x},t)$, the source $f(\theta,\boldsymbol{x},t)$ is square integrable with respect to $\mathbb{P}$, i.e.,

$$\int_0^T\int_D\mathbb{E}\left[f^2\right]d\boldsymbol{x}dt<\infty, \tag{20}$$

and the diffusion coefficient $\mathcal{K}(\theta,\ \boldsymbol{x})$ is uniformly bounded from below, i.e.,

$$\begin{aligned}&\exists\mathcal{K}_{\min}>0\ \text{ such that}\\ &\qquad\mathbb{P}\left(\theta\in\Omega:\mathcal{K}(\theta,\boldsymbol{x})>\mathcal{K}_{\min},\forall\boldsymbol{x}\in\overline{D}\right)=1.\end{aligned} \tag{21}$$

Now, let define the spaces $\mathcal{V}(D)=\{v\in H^1(D)|v=0\text{ on }\Gamma_D\}$ and $V=L^2(0,T;\mathcal{V}(D)\otimes L^2_{\mathbb{P}}(\Omega))$. Thus, we may consider the following weak form of the stochastic initial boundary-value problem:

$$\begin{aligned}&\text{Find } u\in V \text{ with } \partial_t u\in U \text{ such that}\\ &B(u,v)=\mathcal{F}(v)+\int_{\Omega}\int_D u_0v(0)d\boldsymbol{x}d\mathbb{P}(\theta),\quad\forall v\in V,\end{aligned} \tag{22}$$

where now

$$\begin{aligned}B(u,v)&=\int_{\Omega}a(u(\theta,\boldsymbol{x},t),v(\theta,\boldsymbol{x},t))d\mathbb{P}(\theta);\\ \mathcal{F}(v)&=\int_{\Omega}F(v(\theta,\boldsymbol{x},t))d\mathbb{P}(\theta),\end{aligned} \tag{23}$$

with $a(\cdot,\cdot)$ and $F(\cdot)$ given by Eqs. (3) and (8), respectively.

Analogously, the corresponding adjoint problem is

$$\begin{aligned}&\textit{Find } p\in V \textit{ with } \partial_t p\in U \textit{ and } p(T)=0 \textit{ such that}\\ &B(v,p)=\mathcal{Q}(v),\quad\forall v\in V,\end{aligned} \tag{24}$$

where now

$$\mathcal{Q}(v)=\int_{\Omega}Q(v(\theta,\boldsymbol{x},t))d\mathbb{P}(\theta)=\int_{\Omega}\int_0^T\int_{\omega\subset D}\frac{1}{|\omega|}q(v(\theta,\boldsymbol{x},t))d\boldsymbol{x}dtd\mathbb{P}(\theta). \tag{25}$$

4. Karhunen–Loève expansions

A popular construction in the treatment of linear stochastic partial differential equations is to reduce the dimensionality in the random variables through the use of a truncated Karhunen–Loève expansion (see, e.g. [8–11,14]). Let $m(\theta,\ \boldsymbol{x})$ denote a random function with continuous covariance

$$\begin{aligned}&\mathbb{C}ov[m]:\overline{D}\times\overline{D}\to\mathbb{R};\\ &\mathbb{C}ov[m]\left(\boldsymbol{x},\boldsymbol{x}'\right)=\mathbb{E}\left[(m(\cdot,\boldsymbol{x})-\mathbb{E}[m](\boldsymbol{x}))\left(m\left(\cdot,\boldsymbol{x}'\right)-\mathbb{E}[m]\left(\boldsymbol{x}'\right)\right)\right]\end{aligned} \tag{26}$$

and associated variance given by $\mathbb{V}ar[m]=\mathbb{E}[(m-\mathbb{E}[m])^2]$. For each such m, one can define a compact self-adjoint operator from $L^2(D)$ into $C^0(\overline{D})$ by

$$Kv=\int_D\mathbb{C}ov[m]\left(\boldsymbol{x},\boldsymbol{x}'\right)v\left(\boldsymbol{x}'\right)d\boldsymbol{x}'. \tag{27}$$

The operator K possesses a countable set $\{(\lambda_n, \varphi_n)\}_{n=1}^{\infty}$ of eigenvalue–eigenfunction pairs (λ_n, φ_n) such that

$$\begin{aligned}
&\left\{\int_{D\times D}\left|\mathbb{C}ov[m]\left(\boldsymbol{x},\boldsymbol{x}'\right)\right|^2 d\boldsymbol{x}d\boldsymbol{x}'\right\}^{1/2} \geq \lambda_1 \geq \lambda_2 \geq \ldots \geq 0;\\
&\int_D \varphi_i(\boldsymbol{x})\varphi_j(\boldsymbol{x})d\boldsymbol{x} = \delta_{ij};\\
&\sum_{n=1}^{\infty}\lambda_n = \int_D \mathbb{V}ar[m](\boldsymbol{x})d\boldsymbol{x}.
\end{aligned} \tag{28}$$

The truncated Karhunen–Loève expansion of the random function m is then

$$m_N(\theta,\boldsymbol{x}) = \mathbb{E}[m](\boldsymbol{x}) + \sum_{n=1}^{N}\sqrt{\lambda_n}\varphi_n(\boldsymbol{x})Y_n(\theta), \tag{29}$$

where $\{Y_n(\theta)\}_{i=1}^{\infty}$ are real random variables that are mutually uncorrelated, have unit variance, and zero mean. Moreover, for each $\lambda_n>0$, the corresponding random variable Y_n is uniquely determined by

$$Y_n(\theta) = \lambda_n^{-1/2}\int_D (m(\theta,\boldsymbol{x})-\mathbb{E}[m](\boldsymbol{x}))\varphi_n(\boldsymbol{x})d\boldsymbol{x}. \tag{30}$$

One can show (Cf. [14]) that the approximation (29) of m converges to m as $N\to\infty$ in the sense that

$$\lim_{N\to\infty}\left\{\sup_{x\in D}\mathbb{E}\left[(m-m_N)^2\right](\boldsymbol{x})\right\} = 0. \tag{31}$$

It is important to recognize that this property also implies that

$$\lim_{N\to\infty}\left\{\sup_{x\in D}(\mathbb{V}ar[m]-\mathbb{V}ar[m_N])(\boldsymbol{x})\right\} = 0. \tag{32}$$

For practical purposes, the number of terms N of the Karhunen–Loève expansion (29) should be as low as possible according to a preset tolerance, and depends on the decay of the eigenvalues λ_n. A fast decay, generally related to a higher correlation length, indicates a natural anisotropic behavior with respect to the stochastic directions. This effect is exploited in the proposed adaptive algorithm presented in Section 6.

Returning now to Eqs. (22) and (24) (or, formally, to Eqs. (1) and (10)), we make the following additional assumptions:

A.1) the random functions $\boldsymbol{w}(\theta,\boldsymbol{x},t)$, $\mathcal{K}(\theta,\boldsymbol{x})$, and $f(\theta,\boldsymbol{x},t)$ depend only on an N-dimensional random vector $\boldsymbol{Y}$ in the spirit of the KL expansion (29);

A.2) the velocity field $\boldsymbol{w}=\boldsymbol{w}(\theta,\boldsymbol{x},t)$ is solenoidal $\nabla\cdot\boldsymbol{w}$

A.3) the images $Y_n:\Omega\to\mathbb{R}$ are uniformly bounded in $\mathbb{R}$, which means that their images,

$$\Gamma_n = Y_n(\Omega),\quad 1\leq n\leq N,$$

are bounded intervals in $\mathbb{R}$;

A.4) the random vector $\boldsymbol{Y}$ has a bounded probability density $\rho:\prod_{n=1}^{N}\Gamma_n\to[0,\infty)$.

Under these assumptions (Cf. [14]), the probability space $(\Omega,\mathcal{U},\mathbb{P})$ can be replaced by $(\Gamma,\mathcal{B}(\Gamma),\rho(\boldsymbol{y})d\boldsymbol{y})$, $\Gamma\equiv\prod_{n=1}^{N}\Gamma_n$, and the probability distribution measure for $\boldsymbol{Y}$ is then $d\mu_{\boldsymbol{Y}}=\rho(\boldsymbol{y})d\boldsymbol{y}$. The result is that the solution of the stochastic initial boundary-value problem can be replaced by a finite number of random variables, $u(\theta,\boldsymbol{x},t)=u(Y_1(\theta),\ldots,Y_N(\theta),\boldsymbol{x},t)$. Moreover, the spaces V and U in Eq. (18) can be replaced by

$$\begin{aligned}
V &= L^2\left(0,T;\mathcal{V}(D)\otimes L^2_\rho(\Gamma)\right);\\
U &= L^2\left(0,T;H^{-1}(D)\otimes L^2_\rho(\Gamma)\right)
\end{aligned} \tag{33}$$

and Eqs. (22) and (24) can likewise be posed in these spaces with

$$\begin{aligned}
B(u,v) &= \int_\Gamma a(u,v)\rho(\boldsymbol{y})d\boldsymbol{y};\\
\mathcal{F}(v) &= \int_\Gamma F(v)\rho(\boldsymbol{y})d\boldsymbol{y},
\end{aligned} \tag{34}$$

etc.

The weak formulations (22) and (24) may be regarded as space-time formulations, as the test functions v are time dependent. A slightly different formulation can be stated in which the test functions are independent of time and the solution u is a one-parameter family of solutions, with time t the parameter. Then the forward problem is

$$\begin{aligned}
&\text{For a.e. } t\in[0,T],\ \text{find } u(t) = u(\boldsymbol{Y},\boldsymbol{x},t)\in\mathcal{V}(D)\otimes L^2_\rho(\Gamma)\\
&\text{such that } u(0) = u_0 \text{ and a.e. on } [0,T],\\
&\int_{\Gamma\times D}[\partial_t uv + \boldsymbol{w}\cdot\nabla u v + \mathcal{K}\nabla u\cdot\nabla v]d\boldsymbol{x}\rho d\boldsymbol{y}\\
&\quad = \int_{\Gamma\times D} fv d\boldsymbol{x}\rho d\boldsymbol{y} + \int_{\Gamma\times\Gamma_N} gv ds\rho d\boldsymbol{y},\quad \forall v\in\mathcal{V}(D)\otimes L^2_\rho(\Gamma),
\end{aligned} \tag{35}$$

and the backward or adjoint problem is

$$\begin{aligned}
&\text{For a.e. } t\in[0,T],\ \text{find } p(t) = p(\boldsymbol{Y},\boldsymbol{x},t)\in\mathcal{V}(D)\otimes L^2_\rho(\Gamma)\\
&\text{such that } p(T) = 0 \text{ and a.e. on } [0,T],\\
&\int_{\Gamma\times D}[-\partial_t pv - \boldsymbol{w}\cdot\nabla pv + \mathcal{K}\nabla p\cdot\nabla v]d\boldsymbol{x}\rho d\boldsymbol{y}\\
&\quad = \int_{\Gamma\times\omega}|\omega|^{-1}q(v)d\boldsymbol{x}\rho d\boldsymbol{y},\quad \forall v\in\mathcal{V}(D)\otimes L^2_\rho(\Gamma).
\end{aligned} \tag{36}$$

5. Discrete approximations of the forward and backward problems

We now consider discrete approximations of the forward and backward problems (35) and (36) and we explore critical issues connected with their implementations. We will use finite element approximation in space and the stochastic collocation method in the probability domain. The latter is a non-intrusive method which naturally leads to uncoupled deterministic problems [13,16]. This advantage is exploited in the proposed approach.

5.1. Finite element and stochastic collocation methods

To define the approximation spaces, we follow the standard FEM discretization process: the domain D is partitioned into a regular family of N_h subdomains K_i, with $h_{K_i}=diam\{\overline{K}_i\}$. Let $h=\max_{i=1,\ldots,N_h}\{h_{K_i}\}$. Each K_i is the image of a master element $\hat{K}$ under a sequence of affine maps $\{F_i\}_{i=1}^{N_h}$ such that $\overline{D}=\bigcup_{i=1}^{N_h}\overline{K}_i, K_i\cap K_j=\emptyset, i\neq j$. Over $\hat{K}$ we introduce polynomial approximations that contain complete polynomials of degree $\leq k$. The resulting piecewise test functions v_k defined on $\overline{D}$ are in $C^0(D)$ and belong to a subspace $W^h(D)\subset H^1(D)$. We assume that standard interpolation and approximation properties prevail. For example, for D a convex polygonal domain, $k=1$ and a given function $\varphi\in H^1(D)$, we have

$$\min_{v\in W_h(D)}\|\varphi-v\|_{H^1(D)}\leq ch\|\varphi\|_{H^2(D)}, \tag{37}$$

where c is independent of h. We also assume that there is a finite element operator $\pi_h: H^1(D) \to W^h(D)$ such that

$$\|\varphi - \pi_h\varphi\|_{H^1(D)} \le C_\pi \min_{v \in W^h(D)} \|\varphi - v\|_{H^1(D)} \quad \forall \varphi \in H^1(D), \tag{38}$$

where again C_π stands for a constant independent of h. In general, the operator π_h depends on the domain problem as well as on the random variables $Y_n(\theta)$, $n = 1, \ldots, N$ (see [13,19] for more details).

The basic idea of the Stochastic Collocation Method (SCM) is to approximate the multidimensional stochastic space using interpolation functions on a set of points $\{\tilde{\boldsymbol{y}}_j\}_{j=1}^M$, called collocation points [13,16,20]. Let $\mathcal{P}_\rho(\Gamma)$ denote the stochastic discrete space such that $\mathcal{P}_\rho(\Gamma) \subset L^2_\rho(\Gamma)$, which can be constructed on either full or sparse tensor product approximation spaces. Before considering these different choices, we may generally define $\mathcal{P}_\rho(\Gamma) = span\{l_i\}_{i=1}^M$, where $l_i(\tilde{\boldsymbol{y}}_j) = \delta_{ij}$, $1 \le i, j \le M$, are the Lagrange polynomials defined on the points $\{\tilde{\boldsymbol{y}}_j\}_{j=1}^M$. In this way, the global solution of the forward problem (35) (and of the backward problem (36)) $u(\boldsymbol{Y}, \boldsymbol{x}, t) \approx u_{\rho,h}(\boldsymbol{Y}, \boldsymbol{x}, t)$ at $\forall t \in (0, T)$, can be obtained by a linear combination of deterministic solutions at these point values, i.e.,

$$u_{\rho,h}(\boldsymbol{Y}, \boldsymbol{x}, t) = \sum_{j=1}^M u_h\left(\tilde{\boldsymbol{y}}_j, \boldsymbol{x}, t\right) l_j(\boldsymbol{Y}), \tag{39}$$

where $u_h(\tilde{\boldsymbol{y}}_j, \boldsymbol{x}, t) \equiv \pi_h u(\tilde{\boldsymbol{y}}_j, \boldsymbol{x}, t) \in W^h(D)$. This means that the weak formulations (35) and (36) can be now stated such that the test functions are independent of the stochastic direction and the solution u is a two-parameter family of solutions, with time t and the collocation points as parameters. Then, the forward problem is

$$\begin{aligned} &\text{For a.e. } t \in [0,T] \text{ and } \tilde{\boldsymbol{y}}_j, 1 \le j \le M, \\ &\text{find } u_h\left(\tilde{\boldsymbol{y}}_j; t\right) = u_h\left(\tilde{\boldsymbol{y}}_j; \boldsymbol{x}, t\right) \in W^h(D) \\ &\quad \text{such that } u_h(0) = u_0 \text{ and a.e. on } [0,T], \\ &\quad B_j\left(u_h\left(\tilde{\boldsymbol{y}}_j; t\right), v_h\right) = \mathcal{F}_j(v_h), \quad \forall v_h \in W^h(D), \end{aligned} \tag{40}$$

where

$$\begin{aligned} B_j(u_h, v_h) &= \int_D [\partial_t u_h\left(\tilde{\boldsymbol{y}}_j; t\right) v_h + \boldsymbol{w} \cdot \nabla u_h\left(\tilde{\boldsymbol{y}}_j; t\right) v_h \\ &\quad + \mathcal{K} \nabla u_h\left(\tilde{\boldsymbol{y}}_j; t\right) \cdot \nabla v_h] d\boldsymbol{x}; \\ \mathcal{F}_j(v_h) &= \int_D f\left(\tilde{\boldsymbol{y}}_j; t\right) v_h d\boldsymbol{x} + \int_{\Gamma_N} g v_h ds. \end{aligned} \tag{41}$$

Likewise, the backward or adjoint problem is

$$\begin{aligned} &\text{For a.e. } t \in [0,T] \text{ and } \tilde{\boldsymbol{y}}_j, 1 \le j \le M, \text{ find} \\ &p_h\left(\tilde{\boldsymbol{y}}_j; t\right) = p_h\left(\tilde{\boldsymbol{y}}_j, \boldsymbol{x}, t\right) \in W^h(D) \\ &\quad \text{such that } p_h(T) = 0 \text{ and a.e. on } [0,T], \\ &\quad B_j\left(v_h, p_h\left(\tilde{\boldsymbol{y}}_j; t\right)\right) = Q(v_h), \quad \forall v \in W^h(D), \end{aligned} \tag{42}$$

where

$$\begin{aligned} B_j\left(v_h, p_h\left(\tilde{\boldsymbol{y}}_j; t\right)\right) &= \int_D \left[-\partial_t p_h\left(\tilde{\boldsymbol{y}}_j; t\right) v_h - \boldsymbol{w} \cdot \nabla p_h\left(\tilde{\boldsymbol{y}}_j; t\right) v_h \right. \\ &\quad \left. + \mathcal{K} \nabla p_h\left(\tilde{\boldsymbol{y}}_j; t\right) \cdot \nabla v_h\right] d\boldsymbol{x}; \\ Q(v_h) &= \int_\omega |\omega|^{-1} q(v_h) d\boldsymbol{x}. \end{aligned} \tag{43}$$

Once we have the approximation $u_{\rho,h}(\boldsymbol{Y}, \boldsymbol{x}, t)$ in terms of the random inputs $\boldsymbol{Y}$, we may obtain relevant statistical information in a straightforward manner. The mean solution, for example, is

$$\begin{aligned} \mathbb{E}[u] \approx \mathbb{E}\left[u_{\rho,h}\right] &= \sum_{j=1}^M u_h\left(\tilde{\boldsymbol{y}}_j; t\right) \int_\Gamma l_j(\boldsymbol{Y}) \rho(y) dy \\ &\approx \sum_{j=1}^M u_h\left(\tilde{\boldsymbol{y}}_j; t\right) w_j, \end{aligned} \tag{44}$$

where w_j are the weights associated with the cubature rule associated with the collocation points.

5.2. Choices of collocation points

The SCM is based on polynomial approximations of the solutions in the $\boldsymbol{y} \in \Gamma^N$ (random representable) variables and determining those polynomials by specifying some points in the random space where the approximate solution is determined. One goal is to locate these points appropriately so as to achieve the desired accuracy. The points are chosen to be a set of cubature points so that when integrals are replaced by a discrete sum, as in Eq. (44), the weights are explicitly known, thus avoiding explicit evaluations of the Lagrange polynomials [18].

To define the full tensor product interpolation, we first consider $u \in C^0(\Gamma^1; W(D))$ and $N = 1$. A sequence of one-dimensional Lagrange interpolation operators $\mathcal{U}^i: C^0(\Gamma^1; W(D)) \to V_{m_i}(\Gamma^1; W(D))$ is given by (cf. [14])

$$\mathcal{U}^i(u)(y) = \sum_{j=1}^{m_i} u\left(y_j^i\right) l_j^i(y), \tag{45}$$

where $l_j^i(y) \in \mathbb{P}_{m_i - 1}(\Gamma^1)$ are the Lagrange polynomials of degree $m_i - 1$ and

$$\begin{aligned} &V_{m_i}\left(\Gamma^1; W(D)\right) \\ &\quad = \left\{ v \in C^0\left(\Gamma^1; W(D)\right) : v(y, \boldsymbol{x}) = \sum_{j=1}^{m_i} \tilde{v}_j(\boldsymbol{x}) l_j^i(y), \left\{\tilde{v}_j\right\}_{j=1}^{m_i} \in W(D) \right\}. \end{aligned} \tag{46}$$

The superscript i in Eq. (45) defines the accuracy of the formula, being exact for polynomials of degree less than m_i. For $N > 1$, a vector-index $\boldsymbol{i} = (i_1, \ldots, i_N) \in \mathbb{N}_+^N$ is used to define a full tensor interpolation formula

$$\begin{aligned} \mathcal{U}^{\boldsymbol{i}}(u)(\boldsymbol{y}) &= (\mathcal{U}^{i_1} \otimes \cdots \otimes \mathcal{U}^{i_N})(u)(\boldsymbol{y}) \\ &= \sum_{j_1=1}^{m_1} \cdots \sum_{j_N=1}^{m_N} u\left(y_{i_1}, \cdots, y_{i_N}\right) \left(l_{j_1}^{i_1} \otimes \cdots \otimes l_{j_N}^{i_N}\right). \end{aligned} \tag{47}$$

As shown in this formula, different numbers of points may be used in each direction and the total number of points is given by $M = \prod_{n=1}^N m_n$. As N increases, M quickly becomes very large. To avoid this "curse of dimensionality", the Smolyak sparse grid technique may be used [21–23], which starts from the previous full tensor product representation and discards some multi-indices to construct the minimal representation of the function while preserving the desired accuracy. The Smolyak algorithm builds the interpolation function $\mathcal{U}_{q,N}$ (where $q \in \mathbb{N}_+$ and $q - N$ is the order of interpolation) by using a combination of one-dimensional functions with index i_n, $n = 1, \ldots, N$, with the constraint that the total sum ($|\boldsymbol{i}| = i_1 + \ldots + i_N$) across all dimensions is between $q - N + 1$ and q, i.e.,

$$\mathcal{U}_{q,N}(u)(\boldsymbol{y}) = \sum_{q-N+1 \le |i| \le q} (-1)^{q-|\boldsymbol{i}|} \binom{N-1}{q-|\boldsymbol{i}|} \left(\mathcal{U}^{i_1} \otimes \ldots \otimes \mathcal{U}^{i_N}\right)(u)(\boldsymbol{y}). \tag{48}$$

As q is increased, more points are sampled. The multivariate index $\boldsymbol{i}$ may also be defined by the index set

$$X(q,N) := \left\{ i \in \mathbb{N}_+^N,\ i \geq 1 \ :\ \sum_{n=1}^{N} (i_n - 1) \leq q \right\}. \tag{49}$$

To compute $\mathcal{U}_{q,N}(u)(\boldsymbol{y})$ it is only necessary to know the solution values at the sparse grid

$$\mathcal{H}_{q,N} = \bigcup_{q-N+1 \leq |i| \leq q} \left(\Theta^{i_1} \times \ldots \times \Theta^{i_N} \right),$$

where $\Theta^{i_n} \{ y_1^{i_n}, \ldots, y_{m_{i_n}}^{i_n} \} \subset \Gamma^n$ denotes the set of points used by the one-dimensional formula $\mathcal{U}^{i_n}$. Define now the differential (incremental) operator

$$\Delta^i := \mathcal{U}^i - \mathcal{U}^{i-1}, \tag{50}$$

with $\mathcal{U}^0 = 0$. Then

$$\begin{aligned} \mathcal{U}_{q,N}(u)(\boldsymbol{y}) &= \sum_{|\boldsymbol{i}| \leq q} \left(\Delta^{i_1} \otimes \ldots \otimes \Delta^{i_N} \right)(u)(\boldsymbol{y}) \\ &= \mathcal{U}_{q-1,N}(u)(\boldsymbol{y}) + \sum_{|\boldsymbol{i}| \leq q} \left(\Delta^{i_1} \otimes \ldots \otimes \Delta^{i_N} \right)(u)(\boldsymbol{y}). \end{aligned} \tag{51}$$

Thus, to extend the interpolation from level $q-1$ to q, we only need to evaluate the differential formula. By choosing a one-dimensional formula based on nested points, such as Chebyshev and Gauss–Lobatto points, the solution has to be evaluated at the grid points that are unique to level q , defined as $\Theta_\Delta^i = \Theta^i \backslash \Theta^{i-1}$, so that the differential nodes lie in a set $\Delta\mathcal{H}_{q,N}$ given by

$$\Delta\mathcal{H}_{q,N} = \bigcup_{|\boldsymbol{i}| = q} \left(\Theta_\Delta^{i_1} \times \ldots \times \Theta_\Delta^{i_N} \right). \tag{52}$$

The Smolyak formulas (Eq. (48)) are particularly useful whenever nested points are used since they permit the evaluation of the error based on the difference of two subsequent formulas [23,24]. For such situations, it is proved in [21] that the Smolyak formula is actually interpolatory.

The Smolyak's formulas that are based on polynomial interpolation at the extrema of the Chebyshev polynomials was first used in [16] in the context of SCM. Nobile et al. have analyzed in [19] the Smolyak's approximation error for elliptic problems by assuming that the solution depends analytically on each random variable. Algebraic convergence rates are obtained in these situations, but the exponent of the algebraic convergence also depends on the dimension of the probabilistic space N. To avoid this drawback, anisotropic formulas may be used [15,25,26]. They are constructed by defining an N-dimensional weight vector $\boldsymbol{\alpha} = (\alpha_1, \ldots, \alpha_N) \in \mathbb{R}_+^N$ such that the anisotropic rule is

$$U_{q,N}^{\alpha}(u)(\boldsymbol{y}) = \sum_{\boldsymbol{i} \in X_\alpha(q,N)} \left(\Delta^{i_1} \otimes \ldots \otimes \Delta^{i_N} \right)(u)(\boldsymbol{y}) \tag{53}$$

where the index set is defined by

$$X_\alpha(q,\mathbb{N}) := \left\{ \boldsymbol{i} \in \mathbb{N}_+^N, \boldsymbol{i} \geq 1 \ :\ \sum_{n=1}^{N} (i_n - 1)\, \alpha_n \leq \underline{\alpha}_q \right\} \tag{54}$$

and $\underline{\alpha} = \min_{1 \leq n \leq N} \alpha_n$. The weight factors α_n are supposed to treat each stochastic direction differently, assigning fewer collocation points in direction n when α_n is higher, taking advantage of some specific solution structure to reduce the total number of collocation points. In this work, we construct the weight vector $\boldsymbol{\alpha} = (\alpha_1, \ldots, \alpha_N)$ to adjust the probabilistic grid so as to control the approximation error of a quantity of interest.

5.3. Some implementation issues

The solutions of Eqs. (40) and (42) by using the Galerkin method may lose coercivity when the advection phenomenon dominates the transport. Such numerical difficulties are due to the presence of considerable information contained in small scales and whose effects are not represented on the large scales, giving rise to the spurious modes which may pollute the entire solution. To rectify these difficulties, different methodologies have been developed in the literature, which, in some sense, end up on adding a regularization term to the Galerkin form (Cf. [27]). For the forward problem, the formulation becomes:

$$\begin{aligned} &\textit{For a.e. } t \in [0,T] \textit{ and } \tilde{\boldsymbol{y}}_j,\ 1 \leq j \leq M, \textit{ find} \\ &u_h\left(\tilde{\boldsymbol{y}}_j; t\right) = u_h\left(\tilde{\boldsymbol{y}}_j; \boldsymbol{x}, t\right) \in W^h(D) \\ &\textit{such that } u_h(0) = u_0 \textit{ and a.e. on } [0,T], \\ &B_j\left(u_h\left(\tilde{\boldsymbol{y}}_j; t\right), v_h\right) + \mathcal{R}_j\left(u_h\left(\tilde{\boldsymbol{y}}_j; t\right), v_h\right) = \mathcal{F}_j(v), \quad \forall v \in W^h(D). \end{aligned} \tag{55}$$

The model term $\mathcal{R}_j(u_h(\tilde{\boldsymbol{y}}_j;\ t),\ v_h)$ depends on the weighting function v_h, the trial function $u_h(\tilde{\boldsymbol{y}}_j;\ t)$ and may depend on the input data. It usually depends on the characteristic spatial mesh size h and may also depend on one or more user-specified parameters τ. Different models yield different methods. Regarding stabilized finite element methods, the SUPG method [28] in the present stochastic collocation approach leads to a regularization which is given by

$$\mathcal{R}_j(u_h\left(\tilde{\boldsymbol{y}}_j; t\right), v_h) = \sum_{i=1}^{N_h} \left(A u_h\left(\tilde{\boldsymbol{y}}_j; t\right) - f, \tau \boldsymbol{w}\left(\tilde{\boldsymbol{y}}_j\right) \cdot \nabla v_h \right)_{K_i}, \tag{56}$$

where $(\cdot,\cdot)_{K_i}$ denotes the L^2 -inner product defined in $K_i \subset D$. For one-dimensional steady-state advection dominated advection–diffusion problems with no source term and constant input data, the SUPG solution with continuous piecewise linear elements on a uniform partition of the domain is nodally exact if

$$\tau = \frac{h}{2\left|\boldsymbol{w}\left(\tilde{\boldsymbol{y}}_j\right)\right|} \xi\left(Pe\left(\tilde{\boldsymbol{y}}_j\right)\right), \text{ with } \xi\left(Pe\left(\tilde{\boldsymbol{y}}_j\right)\right) = \coth\left(Pe\left(\tilde{\boldsymbol{y}}_j\right)\right) - \frac{1}{Pe\left(\tilde{\boldsymbol{y}}_j\right)}, \tag{57}$$

where the local Peclet number at each collocation point is given by $Pe(\tilde{\boldsymbol{y}}_j) = 0.5\, h\, |\, \boldsymbol{w}(\tilde{\boldsymbol{y}}_j)\, | / \mathcal{K}(\tilde{\boldsymbol{y}}_j)$. For simplicity we use the SUPG method in this work to stabilize the Galerkin formulation for the forward problem (40), as given by Eqs. (55) and (56).

The backward problem (42) has similar structure to the primal problem, with negative velocity field and needs to be solved backward in time. By introducing a transformation of variables $\zeta = T - t$, the backward problem (42) can be recast as the following forward problem:

$$\begin{aligned} &\textit{For a.e. } \zeta \in [0,T] \textit{ and } \tilde{\boldsymbol{y}}_j,\ 1 \leq j \leq M, \textit{ find} \\ &p_h\left(\tilde{\boldsymbol{y}}_j; \zeta\right) = p_h\left(\tilde{\boldsymbol{y}}_j, \boldsymbol{x}, \zeta\right) \in W^h(D) \\ &\textit{such that } p_h(0) = 0 \textit{ and a.e. on } [0,T] \\ &\int_D \left[\partial_\zeta p_h\left(\tilde{\boldsymbol{y}}_j; \zeta\right) v_h - \boldsymbol{w} \cdot \nabla p_h\left(\tilde{\boldsymbol{y}}_j; \zeta\right) v_h + \mathcal{K} \nabla p_h\left(\tilde{\boldsymbol{y}}_j; \zeta\right) \cdot \nabla v_h \right] d\boldsymbol{x} \\ &\quad = Q(v_h), \quad \forall v \in W^h(D). \end{aligned} \tag{58}$$

The weak form Eq. (58) also lacks coercivity when $Pe(\tilde{y}_j)>1$, so that the following regularization term must be added to improve stability:

$$\begin{aligned}\mathcal{R}_j^d\left(p_h\left(\tilde{y}_j;t\right),v_h\right) &= \sum_{i=1}^{N_h}\left(\partial_\zeta p_h\left(\tilde{y}_j;\zeta\right)\right.\\ &\left.-\boldsymbol{w}\cdot\nabla p_h\left(\tilde{y}_j;\zeta\right)v_h-\nabla\cdot\mathcal{K}\nabla p_h\left(\tilde{y}_j;\zeta\right)-q,-\tau\,\boldsymbol{w}\left(\tilde{y}_j\right)\cdot\nabla v_h\right)_{K_i}.\end{aligned} \tag{59}$$

Now, let the time domain $(0,T)$ be divided into subintervals $I_n=(t_{n-1}, t_n)$, $n=1,\ldots,N_T$, where N_T is the total number of subintervals. The time step is $\Delta t=t_n-t_{n-1}$. Let $\{N_a\}_{a=1}^{Np}$ denote the basis functions of $W_h(D)$ so that $u_h(\tilde{y}_j;t)=\sum_{a=1}^{N_p}u_a^jN_a$ and $\partial_t u_h\left(\tilde{y}_j;t\right)=\sum_{a=1}^{N_p}u_a^j\,\partial_t N_a$. We define $\mathbf{u}_h^j:=\left\{u_1^j,\ldots,u_{N_p}^j\right\}^t$ as the vector of unknowns and $\dot{\mathbf{u}}_h^j$ as the time derivative of $\mathbf{u}_h^j$. These definitions allow to recast the system of ordinary Eq. (55) in the following matrix form

$$\mathbf{M}\dot{\mathbf{u}}_h^j+\mathbf{K}\mathbf{u}_h^j=\mathbf{F}, \tag{60}$$

with $\mathbf{M}=[M_{ab}]$, $\mathbf{K}=[K_{ab}]$ and $\mathbf{F}=\{F_a\}$, where

$$M_{ab}=\left(N_a+\tau\boldsymbol{w}\left(\tilde{y}_j\right)\cdot\nabla N_a,N_b\right); \tag{61}$$

$$\begin{aligned}K_{ab} &= \left(N_a,\boldsymbol{w}\left(\tilde{y}_j\right)\cdot\nabla N_b\right)+\left(\nabla N_a,\mathcal{K}\left(\tilde{y}_j\right)\nabla N_b\right)\\ &+\left(\tau\boldsymbol{w}\left(\tilde{y}_j\right)\cdot\nabla N_a,\boldsymbol{w}\left(\tilde{y}_j\right)\cdot\nabla N_b\right)\\ &+\sum_{i=1}^{N_h}\left(\tau\,\boldsymbol{w}\left(\tilde{y}_j\right)\cdot\nabla N_a,-\mathcal{K}\left(\tilde{y}_j\right)\Delta N_b\right)_{K_i};\end{aligned} \tag{62}$$

$$F_a=\left(N_a+\tau\boldsymbol{w}\left(\tilde{y}_j\right)\cdot\nabla N_a,f\right)+(N_a,g)_{\Gamma_N}. \tag{63}$$

We may solve Eq. (60) by using the generalized trapezoidal family of methods yielding the following two-level scheme:

$$(\mathbf{M}+\gamma\Delta t\mathbf{K})\mathbf{u}_h^{j;n+1}=(\mathbf{M}-(1-\gamma)\Delta t\mathbf{K})\mathbf{u}_h^{j;n}+\Delta t\mathbf{F}^{n+\gamma}, \tag{64}$$

where $\gamma\in[0,1]$ is a parameter that defines the integration-in-time method. There are some well known methods derived from Eq. (64): Explicit Euler ($\gamma=0$), Crank–Nicolson ($\gamma=1/2$) and Implicit Euler ($\gamma=1$). The Crank–Nicolson method is used with Δt small enough so that the error due to discretization in time may be disregarded. The same approach is used for the time discretization of the weak dual problem (Eqs. (58) and (59)).

6. Goal-oriented error estimation

We want to assess the accuracy of a quantity of interest associated with the approximate stochastic solution $u(\theta,\boldsymbol{x},T)\approx u_{\rho,h}(\boldsymbol{Y},\boldsymbol{x},T)$, which may be evaluated as

$$\begin{aligned}\mathcal{Q}(u) &= \int_\Gamma\int_0^T\int_{\omega\subset D}\frac{1}{|\omega|}q(u(\theta,\boldsymbol{x},T))d\boldsymbol{x}dt\,\rho(\boldsymbol{y})d\boldsymbol{y}\\ &\approx\int_\Gamma\int_0^T\int_{\omega\subset D}\frac{1}{|\omega|}q\left(u_{\rho,h}(\mathbf{Y},\boldsymbol{x},t)\right)d\boldsymbol{x}dt\,\rho(\boldsymbol{y})d\boldsymbol{y}\\ &=\sum_{j=1}^M\int_0^T\int_{\omega\subset D}\frac{1}{|\omega|}q\left(u_h\left(\tilde{y}_j,\boldsymbol{x},t\right)\right)d\boldsymbol{x}dt\int_\Gamma l_j(\boldsymbol{y})\rho(\boldsymbol{y})d\boldsymbol{y}\\ &=\sum_{j=1}^M\left\{\int_0^T\int_{\omega\subset D}\frac{1}{|\boldsymbol{\omega}|}\sum_{j=1}^M q\left(u_h\left(\tilde{y}_j,\boldsymbol{x},t\right)\right)d\boldsymbol{x}dt\right\}\boldsymbol{w}_j\\ &=\sum_{j=1}^M Q\left(u_h^j\right)\underline{w_j},\end{aligned} \tag{65}$$

in which we approximate the integral on the probabilistic space by using the same cubature rule as used to define the Lagrange interpolation points, so that $\underline{w_j}$ are the weights corresponding to the collocation points $\tilde{y}_j$. This quantity is the expected value of the quantity of interest. Obviously, as we are interested in the solution of a stochastic problem, we are indeed interested in the probability distribution of the solution, and not just its mean. Actually, we want to evaluate such probability distribution as accurately as possible.

On the other hand, as we are approaching the stochastic problem by sampling it at specific collocation points, it seems reasonable to assess the accuracy of the quantity of interest for each of those points and then to recover the desired moments and associated distribution. Thus, for each sampling point $\tilde{y}_j$, $1\le j\le M$, there will be pointwise values $u^j=u(\tilde{y}_j,\boldsymbol{x},t)$. We introduce the following quantity of interest:

$$Q\left(u^j\right)\equiv Q\left(u;\tilde{y}_j,\boldsymbol{x},t\right)=\frac{1}{|\omega|}\int_0^T\int_\omega q\left(u\left(\tilde{y}_j,\boldsymbol{x},t\right)\right)d\boldsymbol{x}dt. \tag{66}$$

This means that we have M estimates of the quantity of interest $Q(u^j), 1\le j\le M$, denoted by $Q(u_h^j)$, which are associated with the corresponding deterministic problems. The following relations establish an a posteriori error estimate for the quantity of interest.

Theorem 1. *Let (u^j,p^j) be the solutions of the forward and adjoint problems*

$$\begin{aligned}&B_j\left(u\left(\tilde{y}_j;t\right),v\right)=\mathcal{F}_j(v),\quad\forall v\in W;\\ &B_j\left(v,p\left(\tilde{y}_j;t\right)\right)=Q(v_h),\quad\forall v\in W,\end{aligned} \tag{67}$$

and let the discrete approximations of these equations be given by

$$\begin{aligned}&B_j\left(u_h\left(\tilde{y}_j;t\right),v_h\right)=\mathcal{F}_j(v_h),\quad\forall v_h\in W^h;\\ &B_j\left(v_h,p_h\left(\tilde{y}_j;t\right)\right)=Q(v_h),\quad\forall v_h\in W^h,\end{aligned} \tag{68}$$

where Q defines the quantity of interest. Then

$$Q\left(u^j\right)-Q\left(u_h^j\right)=B_j\left(e_h^j,\varepsilon_h^j\right)=R_j\left(u_h^j;p^j\right) \tag{69}$$

where

$$e_h^j=u^j-u_h^j\quad\text{and}\quad\varepsilon_h^j=p^j-p_h^j \tag{70}$$

and $R_j(\cdot,\cdot)$ is the residual functional,

$$R_j(v;z)=\mathcal{F}_j(z)-B_j(v,z). \tag{71}$$

Proof. A straightforward calculation reveals that

$$\begin{aligned}Q\left(u^j\right)-Q\left(u_h^j\right) &= B_j\left(u^j,p^j\right)-B_j\left(u_h^j,p_h^j\right)\\ &=B_j\left(u^j,p^j\right)-B_j\left(u_h^j,p_h^j-p^j+p^j\right)\\ &=B_j\left(u^j,p^j\right)-B_j\left(u_h^j,p^j\right)+B_j\left(u_h^j,p^j-p_h^j\right)\\ &=B_j\left(u^j-u_h^j,p^j-p_h^j\right),\end{aligned} \tag{72}$$

which is the first equality in Eq. (69). Here we have used the Galerkin orthogonality of the errors: $B_j(u^j-u_h^j,p_h^j)=0$, etc. The remaining equality follows from the calculations

$$\begin{aligned} B_j\left(e_h^j,\varepsilon_h^j\right) &= B_j\left(u^j-u_h^j,p^j-p_h^j\right)\\ &= B_j\left(u^j-u_h^j,p^j\right)\\ &= B_j\left(u^j,p^j\right)-B_j\left(u_h^j,p^j\right)\\ &= \mathcal{F}_j\left(p^j\right)-B_j\left(u_h^j,p^j\right)\\ &= R_j\left(u_h^j;p^j\right). \end{aligned} \tag{73}$$

□

This theorem in various forms is fairly well known and versions of it can be found in, for example, [2–6,29].

Since $Q(\cdot)$ is linear, $Q(u^j-u_h^j)=Q(e^j)$. According to [29], as the error e^j can be bounded above by the residual, an estimate of $Q(e^j)$ can be given as

$$\left|Q\left(e^j\right)\right|\approx\eta^j=\sum_{i=1}^{N_h}\eta_{K_i}^j,\text{with }\eta_{K_i}^j=e_{h,K_i}^j\varepsilon_{h,K_i}^j, \tag{74}$$

where e_{h,K_i}^j and ε_{h,K_i}^j are the elementwise contributions to the global norm of the residuals associated with the primal and dual solutions at each collocation point, respectively, as defined in [30]. We now use the same interpolation rule (Eq. (39)) to interpolate η^j in the probabilistic space Γ, so that we derive an estimate to the expected value of the error with respect to the quantity of interest, which is computed by

$$\begin{aligned} \mu_\eta &= \int_\Gamma\left(\sum_{j=1}^M\eta^j l_j(\boldsymbol{y})\right)\rho(\boldsymbol{y})d\boldsymbol{y}\\ &= \sum_{j=1}^M\eta^j\int_\Gamma l_j(\boldsymbol{y})\rho(\boldsymbol{y})d\boldsymbol{y}=\sum_{j=1}^M\eta^j w_j. \end{aligned} \tag{75}$$

Similarly, we define an estimate of the variance of the error with respect to the quantity of interest as

$$\sigma_\eta=\sum_{j=1}^M\left(\eta^j\right)^2w_j-\left(\sum_{j=1}^M\eta^j w_j\right)^2, \tag{76}$$

and $[\sigma_\eta]_{q;N}$ indicates that the estimate σ_η is obtained by using the probabilistic dimension equal to N and associated interpolation level q.

Eq. (75) may also be written as $\mu_\eta=\sum_{i=1}^{N_h}\eta_{K_i}$, where $\eta_{K_i}=\sum_{j=1}^M\eta_{K_i}^j w_j$ represents the elementwise contribution to μ_η. The quantities η_{K_i}, which are actually estimates of the first moments of the error with respect to the quantity of interest at each element K_i, can be used to derive refinement indicators, as shown in the following section.

6.1. Adaptation strategy

The estimates (75) and (76) are now used to guide an adaptive algorithm which adjusts the sparse probabilistic grid as well as the finite element grid so as to control the error with respect to the quantity of interest. We use the available approximations to define the dimension of the probability space, the anisotropic sparse collocation grid and the spatial mesh. Regarding the stochastic approximation, we want to select the dimension N and the interpolation level q to meet preset tolerances. Moreover, we want to treat each stochastic direction differently by a posteriori selection of the weight vector $\boldsymbol{\alpha}\in R_+^N$. The main steps of the algorithm are as follows:

(1) choose N and an initial finite element mesh; determine the relative importance of each random dimension and evaluate the N-dimensional weight vector $\boldsymbol{\alpha}=(\alpha_1,\ldots,\alpha_N)$;
(2) construct an anisotropic sparse grid by using $q\geq 2$;
(3) evaluate $\eta_{|K_i}$ and refine the elements K_i that exhibit error greater than a prescribed tolerance (tol_1) (tol_1 may be taken as a fraction β of $\eta_{|max}=\max_{1\leq j\leq N_h}\left\{\left|\eta_{|K_j}\right|\right\}$); repeat until $\eta_{max}<tol_1$;
(4) using the anisotropic grid (step (2)) and the new adapted spatial mesh (step (3)), increase q until

$$\left|\left[\sigma_\eta\right]_{q;N}-\left[\sigma_\eta\right]_{q-1;N}\right|/\left[\sigma_\eta\right]_{q-1;N}<tol_2; \tag{77}$$

(5) set $\alpha_{N+1}=\alpha_N$ and $N=N+1$;
(6) repeat (2)–(5) until

$$\left|\left[\sigma_\eta\right]_{q;N}-\left[\sigma_\eta\right]_{q;N-1}\right|/\left[\sigma_\eta\right]_{q;N-1}<tol_2. \tag{78}$$

Step (1) is a postprocessing procedure aimed at identifying the relative importance of each random dimension. This knowledge is used to define the N-dimensional weight vector $\boldsymbol{\alpha}=(\alpha_1,\ldots,\alpha_N)\in\mathbb{R}_+^N$ in order to construct the anisotropic grid by using Eq. (54). We link the weights α_n with the change in the estimate of the error with respect to the quantity of interest: the directions in which the largest change in the error occurs when the number of points (level of interpolation) is increased will require more interpolation points (or collocation points). We verified that the median absolute value (MAD) is quite appropriate to measure the statistical dispersion of the error. Thus, for a given N, we first evaluate the estimates η^j of $Q(e^j)$, $j=1,\ldots,M$, through Eq. (74). Based on the posteriori error estimator proposed in [15], this is done for $i_n=(1,\ldots,1,i_n,1,\ldots,1), i_n=2$, for each stochastic direction $n, 1\leq n\leq N$. The MAD is determined for each i_n: we evaluate the median of the data set, denoted by $\hat{\eta}^j$; the residuals are evaluated as $|r^j|_n=|\eta^j-\hat{\eta}^j|_n$, and the respective median absolute deviation is determined by $MAD_n=median\{|r^j|_n\}_{j=1}^M$. The adaptive strategy introduces more points for higher MAD_n so as to equilibrate the MAD_n among all of the stochastic directions. Thus we adopt $\alpha_n=\max_{1\leq j\leq N}(MAD_n)/MAD_n$, which is used to build the anisotropic Smolyak grid with the index set defined by Eq. (54). In step (2), the interpolation level q will be increased until consistent values of the estimates of the first and second moments of $\mathcal{Q}(e)$ are obtained. We anticipate that μ_η is very stable for all cases so that we focus on the estimate of the second moment (σ_η), resulting in condition (77) — step (4).

When the dimension of the probabilistic domain is increased, there is no information about the relative importance of the new added direction on the accuracy of the quantity of interest. One possible way to get this information is to repeat the postprocessing step (step (1)) by including the new stochastic dimension. However, this procedure would produce a large increase in the cost of the adaptive algorithm. On the other hand, based on the Karhunen–Loève expansion of the random inputs, it is natural to assume that the new added direction $N+1$ is at most as important as the direction N. This assumption implies that the weight vector $\boldsymbol{\alpha}\in\mathbb{N}_+^{N+1}$ should have $\alpha_{N+1}=\alpha_N$, which is established in step (5).

The quantities $\eta_{K_i}=\sum_{j=1}^M\eta_{K_i}^j\boldsymbol{w_j}$ are used to derive the refinements in step (3). We emphasize that η_{K_i} is an estimate of the error with respect to the quantity of interest in each finite element K_i, resulting from the approximation in the physical and probabilistic

spaces and assuming that the error in time is disregarded. As specified in [30], an element K_i is a candidate for refinement if

$$\frac{\left|\eta K_i\right|}{\max\limits_{1\le j\le N_h}\left\{\left|\eta K_j\right|\right\}}\ge \beta,$$

where β is a user-prescribed parameter ranging from zero to one. This ratio, like μ_η, does not change very much with a change of the collocation points, so that the refined spatial grid is actually determined only once.

Motivated by the property (32), step (5) of the adaptive strategy adjusts the number of terms in the Karhunen–Loève expansion so as to meet a preset tolerance in the variance of the estimated error with respect to the quantity of interest.

Remark: *The proposed adaptation strategy is very flexible in the sense that its steps might be performed independently, according to the information one* has about the problem. For example, if N is known a priori, steps (1)–(4) may be performed to adapt the mesh size, the stochastic grid and associated interpolation level to meet the preset tolerances in errors in quantities of interest.

7. Numerical experiments

In the following numerical experiments we consider the one-dimensional transport problem given by

$$\frac{\partial u(\mathbf{Y},x,t)}{\partial t}-\frac{\partial}{\partial x}\mathcal{K}(\mathbf{Y},x)\frac{\partial u(\mathbf{Y},x,t)}{\partial x}+w(\mathbf{Y},t)\frac{\partial u(\mathbf{Y},x,t)}{\partial x}=0,(\mathbf{Y},x,t)\in\Gamma^N\times(0,2)\times(0,T],$$

with homogeneous Dirichlet boundary conditions and the initial condition given by

$$u(x,0)=\begin{cases}1, & \text{if } x\in[0.2,0.7];\\ 0, & \text{otherwise.}\end{cases}$$

We assume that the quantity of interest is

$$\mathcal{Q}(u;x_0)=\int_\Gamma\int_0^T\int_D u(\mathbf{Y},x,t)k\epsilon(x-x_0)dxdt\rho(y)dy,$$

with $x_0=1.2$ and $T=0.6$. The mollifier k_ϵ is chosen as

$$k_\epsilon(x)=\begin{cases}C\exp\left[\dfrac{\epsilon^2}{|x|^2-\epsilon^2}\right], & \text{if } |x|b\,\epsilon;\\ 0, & \text{if } |x|\ge\epsilon.\end{cases}$$

We set $C=2.2523/\epsilon$ and $\epsilon=h/8$ as indicated in [2].

In the following numerical experiments, the initial spatial discretization is obtained by dividing the computational domain into 40 uniform finite elements. The Crank–Nicolson method is used in time with $\Delta t=3.0\times10^{-4}$, which allow us to disregard the error due to discretization in time.

7.1. Case 1: a random diffusivity parameter

We first consider the case in which the uncertainty arises from a random diffusivity parameter, which is modeled by a stationary process with covariance function

$$\mathbb{C}ov\left(x,x'\right)=\mathbb{C}ov\left(x-x'\right)=\sigma^2\exp\left\{-\frac{\left|x-x'\right|^2}{L_c^2}\right\},\tag{79}$$

where $x,x'\in\overline{\mathrm{D}}=[0,2]$, σ^2 is the variance of the random variable and L_c is the correlation length. This process can be approximated by

$$\mathcal{K}(\boldsymbol{y},x)=\mathbb{E}[\mathcal{K}]+\sigma\sqrt{\lambda_0}\varphi_0(x)Y_0+\sum_{n=1}^{\hat{N}}\sigma\sqrt{\lambda_n}\left[\varphi_n(x)Y_{2n-1}+\hat{\varphi}_n(x)Y_{2n}\right]\tag{80}$$

where $\lambda_0=\frac{1}{4}\sqrt{\pi}L_c,\varphi_0(x)=1$ and, for $n=1,\ldots,$

$$\lambda_n=\frac{1}{2}\sqrt{\pi}L_c exp\left\{-\frac{(n\pi L_c)^2}{16}\right\};\quad \varphi_n(x)=cos\left(\frac{1}{2}n\pi x\right);\ \hat{\varphi}_n(x)=sin\left(\frac{1}{2}n\pi x\right).\tag{81}$$

The uncorrelated random variables $Y_n,n=0,\ldots,2\hat{N}$, have zero mean and unit variance. Here we assume that they are independent and uniformly distributed in $[-1,1]$. We also use $\mathbb{E}[\mathcal{K}]=5\times10^{-2},w=1$ and $\sigma=0.001$. This last value guarantees that $\mathcal{K}(\mathbf{Y},x)$ is strictly positive for all N. The covariance function (79), divided by σ^2, is depicted in Fig. 1 for $L_c=0.25$ and 1.0. The associated eigenvalue decays are shown in Fig. 2, which indicate that smaller correlation lengths require more contribution in Eq. (80) from terms associated with smaller eigenvalues.

The first experiment is conducted by using $L_c=1.0$. We start the adaptive algorithm by setting $\hat{N}=2$, which corresponds to use $N=5$.

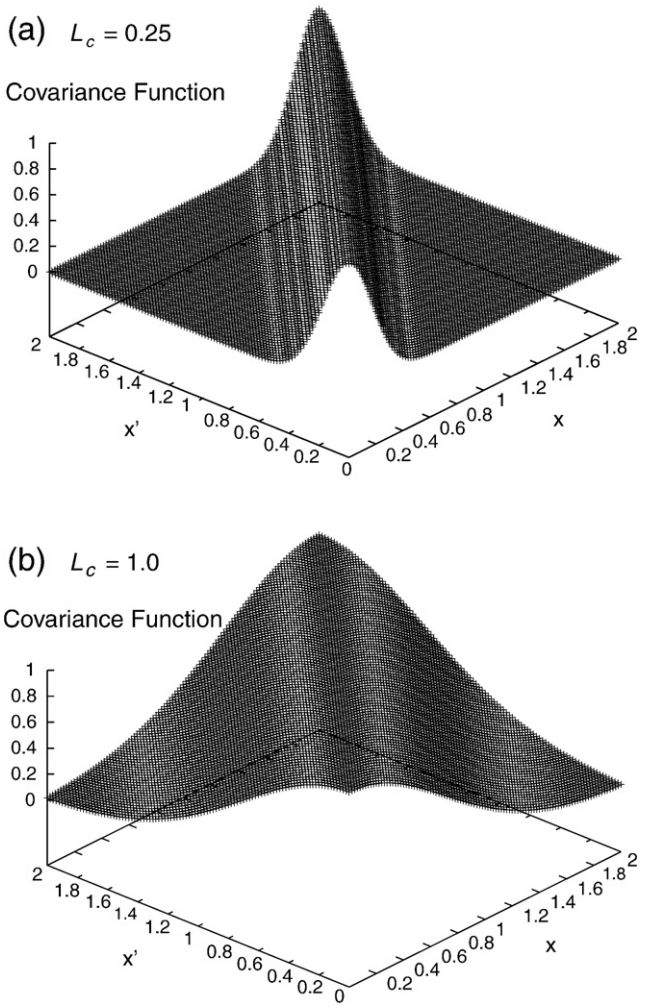

Fig. 1. Exact covariance function versus x and x'; $0\le x\le2,0\le x'\le2$ for $L_c=0.25$ and 1.0.

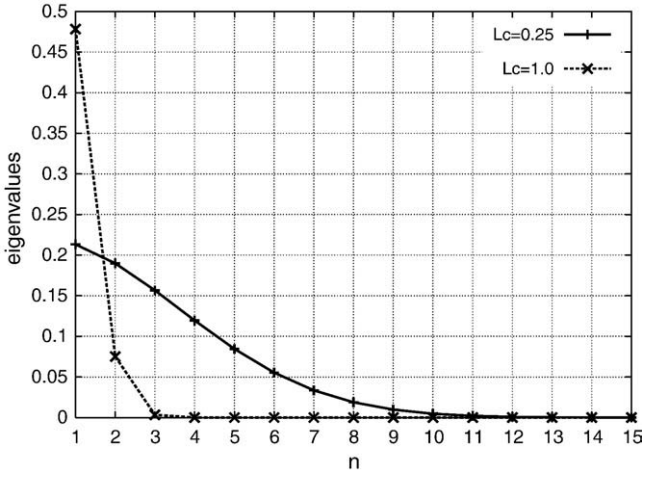

Fig. 2. Eigenvalues λ_n decay, $n=1,2,\ldots$, for $L_c=0.25$ and 1.0.

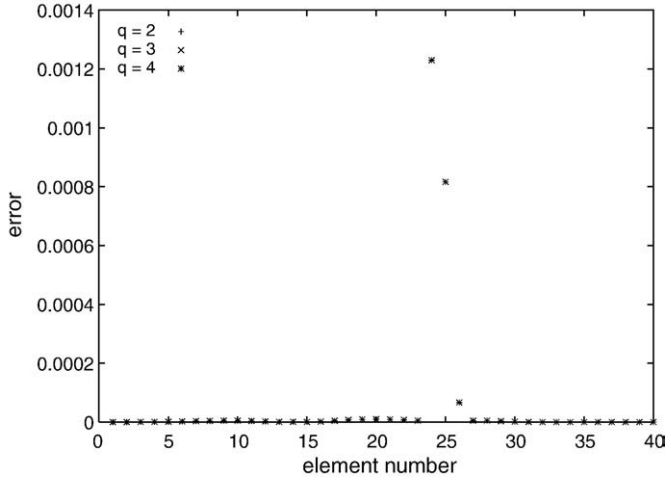

Fig. 3. Elementwise error η_{K_i} for the initial mesh and $2\le q\le 4$.

Table 1 presents the results obtained by evaluating the first step of the algorithm, that is, the identification of the relative importance among the random directions for the initial (coarse) spatial discretization. Table 1 also presents the weight vector and Table 2 shows the associated anisotropic grids for increasing q ($2\le q\le 6$). In this table, the number of grids is the total number of tensor product grids that are used to construct the final grid (see [23] for more details). The proposed strategy is able to capture the solution anisotropy in the probabilistic space. We should point out that this feature is independent of the initial spatial grid. We may also notice that the odd terms in Eq. (80) have stronger effect on the accuracy of the quantity of interest than the even ones. The estimate of the variance of the error with respect to the quantity of interest becomes invariant after $q=4$ (condition (77)). If Smolyak isotropic grids are used for solving the stochastic primal and dual problems, skipping the step 1 of the algorithm, the convergence would be reached for $q=3$. However, the use of anisotropic grids greatly reduces the number of deterministic solvers, which leads to huge computational savings when the problem has an anisotropic behavior with respect to the stochastic directions. In the present case, the isotropic grid would require more than ten times the number of resolutions of deterministic problems than the proposed methodology.

It is also interesting to note that the elementwise contribution η_{K_i} to η, does not change with q, as shown in Fig. 3. This behavior is due to

Table 1
Case 1, $L_c=1.0$: identification of the relative importance among the random directions for $N=5$.

$N=5$		$h=0.05$			α
n	$\boldsymbol{i}_n$	η^j		MAD_n	α_n
1	(2,1,1,1,1)	$j=1$	2.20022E−3	8.07E−6	1.00
		$j=2$	2.20840E−3		
		$j=3$	2.21647E−3		
2	(1,2,1,1,1)	$j=1$	2.21342E−3	5.01E−6	1.60
		$j=2$	2.20840E−3		
		$j=3$	2.20838E−3		
3	(1,1,2,1,1)	$j=1$	2.20601E−3	2.40E−6	3.36
		$j=2$	2.20840E−3		
		$j=3$	2.21083E−3		
4	(1,1,1,2,1)	$j=1$	2.20345E−3	4.96E−6	1.63
		$j=2$	2.20840E−3		
		$j=3$	2.20841E−3		
5	(1,1,1,1,2)	$j=1$	2.21175E−3	3.34E−6	2.42
		$j=2$	2.20840E−3		
		$j=3$	2.20501E−3		

Table 2
Case1, Step 1: anisotropic grids for $2\le q\le 6$.

q	2	3	4	5	6
Number of partial grids	5	9	17	34	55
Number of points	9	23	53	143	323

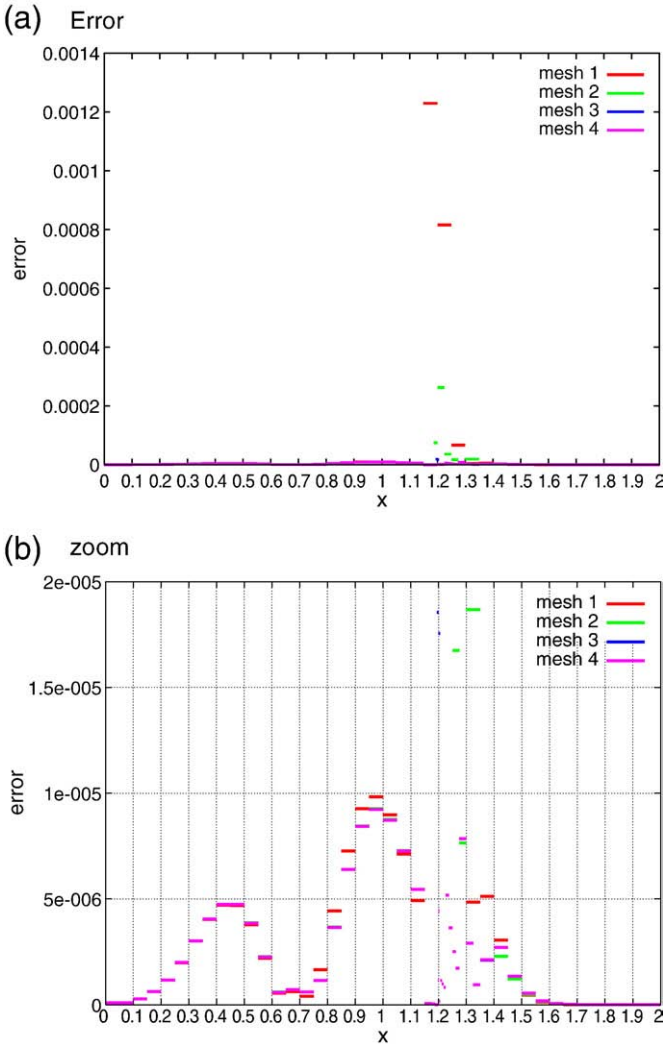

Fig. 4. Error η_{K_i} for all intermediate meshes.

the fact that η_{K_i} are estimates of the first moments of the error with respect to the quantity of interest at each element K_i. Like μ_η, they do not change very much with a change of the collocation points. Thus, we use the anisotropic grid with $q=2$ to reach convergence of η_{K_i}, that is when $\max_{1\le i\le N_h} |\eta_{K_i}| \le tol_1$. Here we use $tol_1 = 10^{-5}$. Fig. 4 shows the error in space for all four intermediate meshes. The partition obtained after four refinements, with 56 elements, is shown in Fig. 5. As expected, the refinement was performed around $x=1.2$.

Using now the final spatial mesh, we increase $\hat{N}$ so that $N=7$ and construct the stochastic grid by using the lower level q for which the estimate of the variance of the error with respect to the quantity of interest becomes invariant. This amounts to using $q=4$. To build the stochastic grid it is also necessary to define the weight vector $\boldsymbol{\alpha}$, although we have no information about the relative importance of the two new stochastic directions on the representation of the quantity of interest. However, we assume that they are at most as important as the last two stochastic directions associated with $\hat{N}=2$. Thus, we set $\alpha_6=\alpha_4$ and $\alpha_7=\alpha_5$ so that the new multidimensional weight vector is $\boldsymbol{\alpha}=(1, 1.6, 3.36, 1.63, 2.42, 1.63, 2.42)$. The addition of two terms of the KLE actually improves the accuracy of the quantity of interest, but the convergence is achieved by increasing $\hat{N}=2$ once more. We also verify that

$$\sup_{x\in D} |\mathbb{V}ar[u_{N=7}] - \mathbb{V}ar[u_{N=9}]|(x) < 10^{-10},$$

where $u_{N=7}$ and $u_{N=9}$ are the primal solutions obtained with a KLE of $\mathcal{K}$ with 7 and 9 terms, respectively. Fig. 6 shows the mean and variance of the primal solution at $t=0.6$. The variance exhibits multi-peak behavior, with the highest peak at the center of the mean and two smaller peaks next to the front and end of the mean profile. Similar multi-peak structure has been reported in [31,32]. The sample histogram of the primal solution at $x=1.2$ (sampling at the collocation points) is shown in Fig. 7. The low amount of sampling points may not be enough to capture the frequency density profile precisely, yielding the observed non-unimodality.

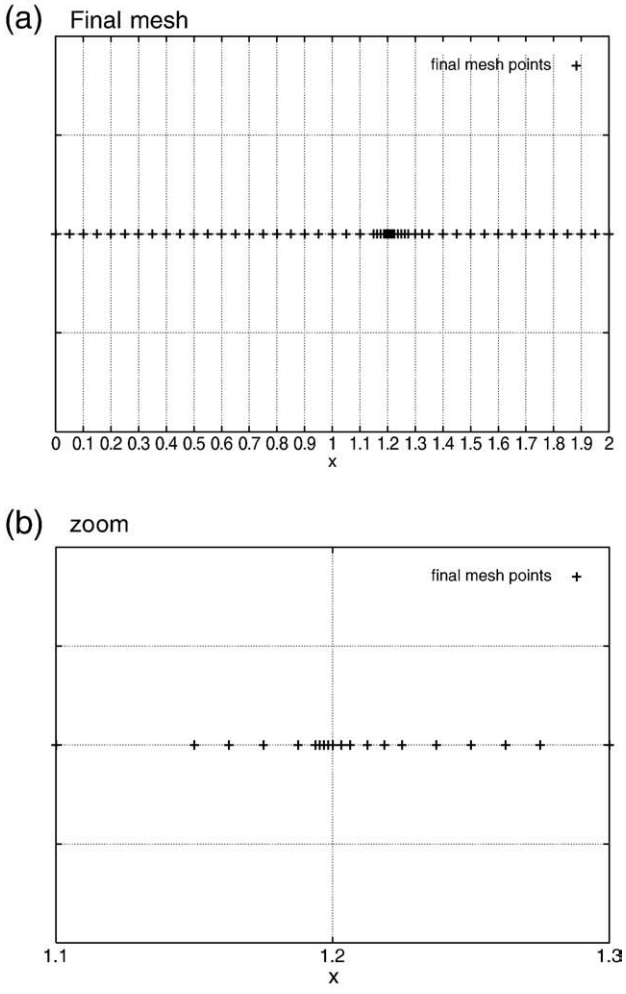

Fig. 5. Final mesh.

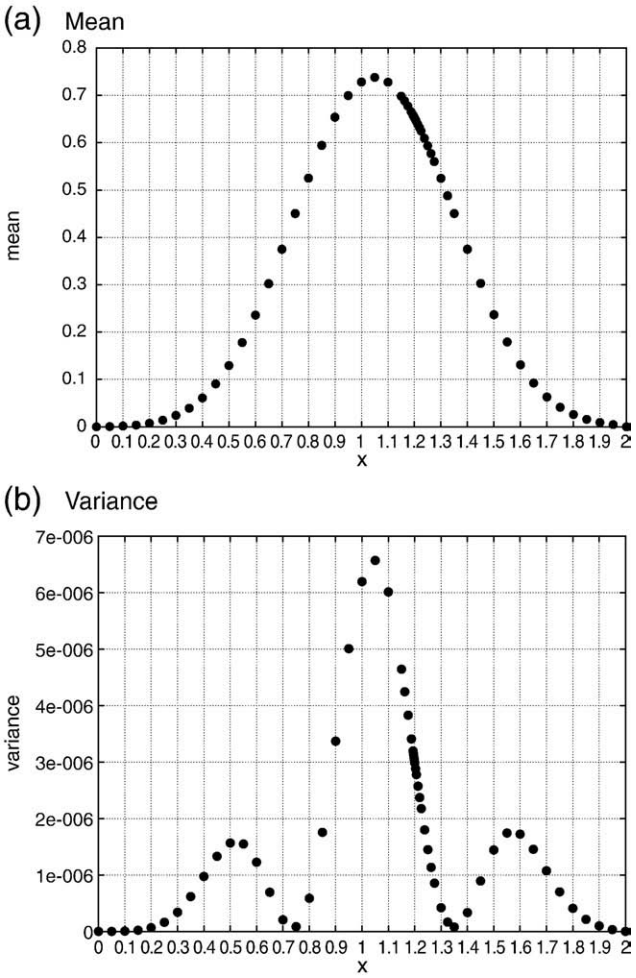

Fig. 6. Mean and variance of the primal solution at $t=0.6$.

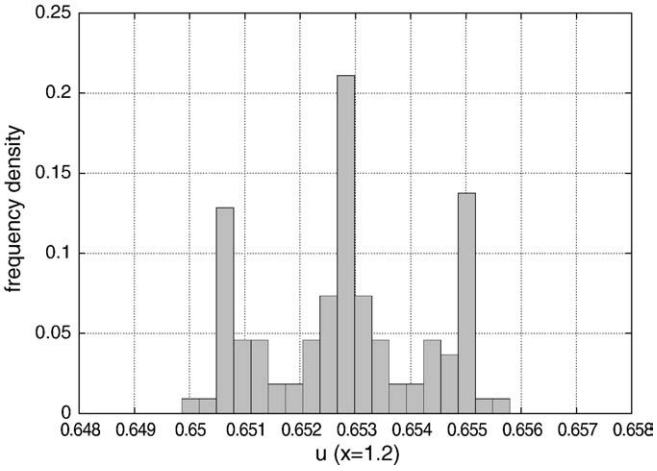

Fig. 7. Histogram of the primal solution at $x=1.2$ and $t=0.6$.

Table 3
Step 5: estimate of the variance of the error $\mathcal{Q}(e)$.

N	*Numb. coll.pts.* $(q=4)$	ϵ_{N+2}	σ_η
3	47	–	3.51515371E−13
5	105	6.03e−07	4.49553011E−13
7	199	2.01e−07	5.37868146E−13
9	337	1.19e−07	8.95593573E−13
11	527	5.75e−08	1.43048523E−12
13	777	2.50e−08	1.78641999E−12
15	1095	1.47e−08	1.11002172E−12
17	1489	9.22e−09	1.11074365E−12
19	1967	5.12e−09	1.11074338E−12

The second experiment is conducted by using $L_c=0.25$, which yields a much slower decay of the eigenvalues of the KLE as compared to the previous experiment (see Fig. 2), so that we expect to have higher stochastic domain dimension than that obtained in the previous experiment. We now start the adaptive algorithm by setting $\widehat{N}=1$, which corresponds to use only $N=3$. The first step of the algorithm yields $\boldsymbol{\alpha}=(1,1.2,2.5)$. As expected, the weight vector indicates a more isotropic behavior than that of the previous case. Step (3) of the algorithm, with $q=2$, yields a refined spatial mesh similar to that obtained in the previous experiment. With the refined spatial mesh, the convergence of the estimate of the variance of the error of the quantity of interest is reached for $q=4$. Next, $\hat{N}=1$ is incrementally increased. The number of points of the associated grids obtained with $\boldsymbol{\alpha}=(1,1.2,2.5,\ldots,1.2,2.5)$ and $q=4$ are indicated in Table 3, which still are much fewer than the number of points required by an isotropic grid. For example, the isotropic approximation with $N=5$ would require 801 collocation points, almost 8 times higher than the proposed anisotropic approximation. The estimate of the variance of the error with respect to the quantity of interest is also shown in Table 3 as well as the error

$$\epsilon_{N+2} = \sup_{x\in D} |\mathbb{V}ar[u_N] - \mathbb{V}ar[u_{N+2}]|(x)$$

regarding the convergence of the primal solution at $t=0.6$ with respect to the dimension of the probability space. Fig. 8 shows the variance of the primal solution at $t=0.6$ as N increases. The mean and variance of the primal solution at $t=0.6$ obtained with $N=19$ is shown in Fig. 9. The corresponding sample histogram of the primal

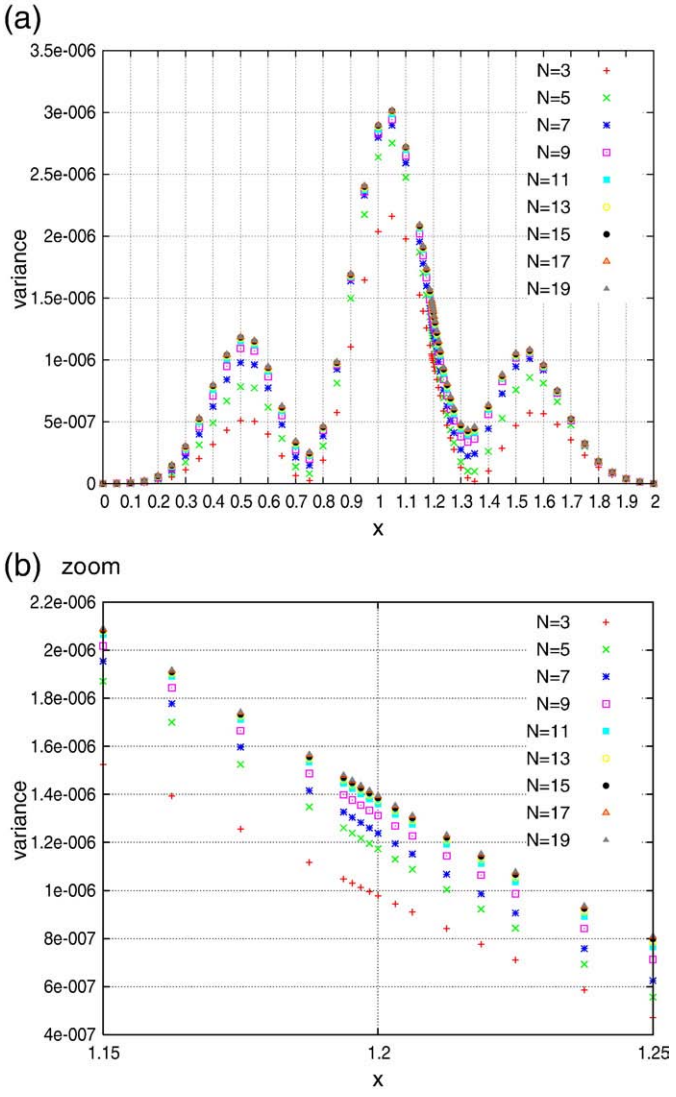

Fig. 8. Variance of the primal solution at $t=0.6$ as N increases.

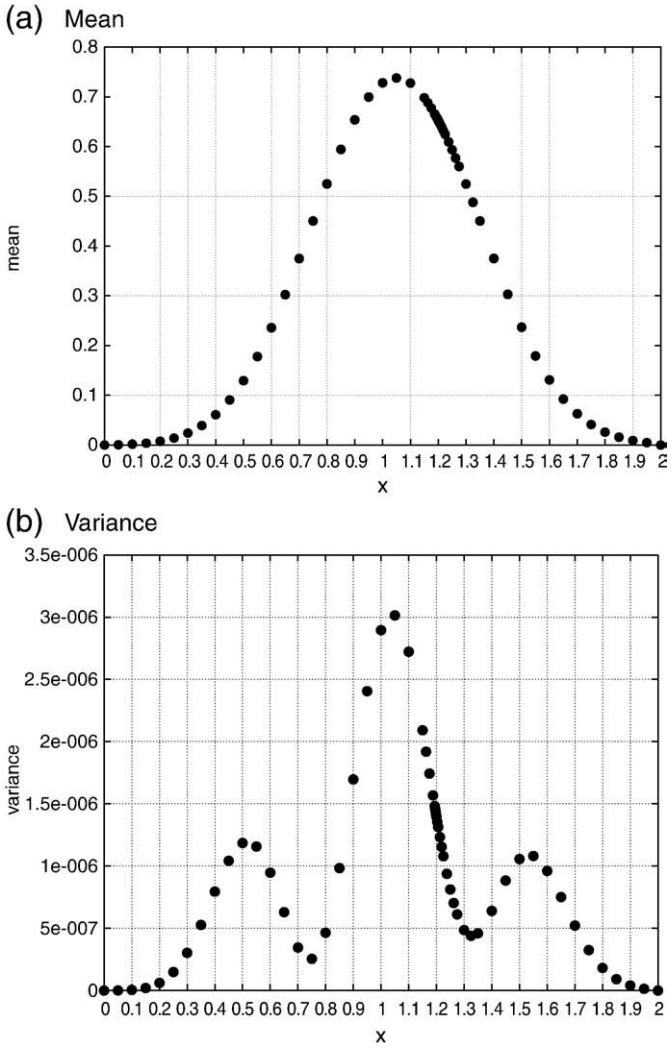

Fig. 9. Mean and variance of the primal solution at $t=0.6$.

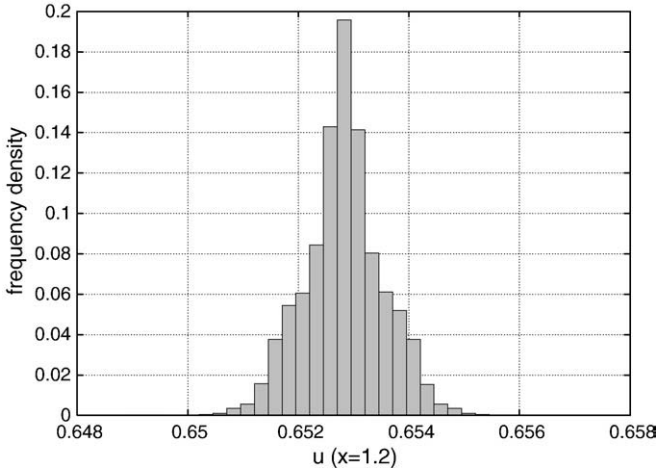

Fig. 10. Histogram of the primal solution at $x = 1.2$ and $t = 0.6$.

solution at $x = 1.2$, sampling at 1967 collocation points, is shown in Fig. 10. The frequency density has a symmetric bell shape profile of a normal distribution.

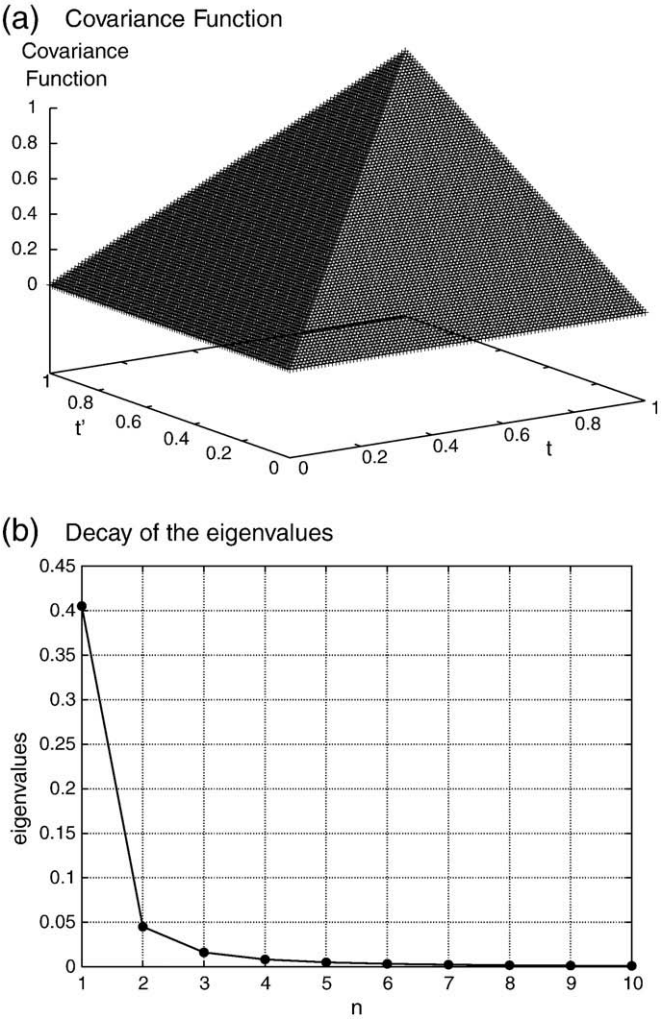

Fig. 11. (a) Exact covariance function versus t and t'; $0 \le t \le 1, 0 \le t' \le 1$; (b) decay of eigenvalues λ_n for the index $n = 1,2, \ldots$.

Table 4
Case 2: identification of the relative importance among the random directions for $N = 3$.

$N=3$		$h=0.05$			α
n	$\boldsymbol{i}_n$	η^j		MAD_n	α_n
1	(2,1,1)	$j=1$	2.10273E−3	1.05E−4	1
		$j=2$	2.20840E−3		
		$j=3$	2.31329E−3		
2	(1,2,1)	$j=1$	2.15632E−3	5.18E−5	2
		$j=2$	2.20840E−3		
		$j=3$	2.26025E−3		
3	(1,1,2)	$j=1$	2.20108E−3	7.31E−6	14
		$j=2$	2.20840E−3		
		$j=3$	2.21571E−3		

Table 5
Case 2: identification of the relative importance among the random directions for $N = 5$ and $i_n = 2$.

$N=5$		$h=0.05$			α
n	$\boldsymbol{i}_n$	η^j		MAD_n	α_n
1	(2,1,1,1,1)	$j=1$	2.10273E−3	1.05E−4	1
		$j=2$	2.20840E−3		
		$j=3$	2.31329E−3		
2	(1,2,1,1,1)	$j=1$	2.15632E−3	5.18E−5	2
		$j=2$	2.20840E−3		
		$j=3$	2.26025E−3		
3	(1,1,2,1,1)	$j=1$	2.20108E−3	7.31E−6	14
		$j=2$	2.20840E−3		
		$j=3$	2.21571E−3		
4	(1,1,1,2,1)	$j=1$	2.20733E−3	1.07E−6	98
		$j=2$	2.20840E−3		
		$j=3$	2.20948E−3		
5	(1,1,1,1,2)	$j=1$	2.20231E−3	6.09E−6	17
		$j=2$	2.20840E−3		
		$j=3$	2.21449E−3		

7.2. Case 2: a random velocity field

We consider now the case in which the uncertainty arises from the random velocity field. The diffusivity parameter is constant and equal

Table 6
Case 2: identification of the relative importance among the random directions for $N = 5$ and $i_n = 3$.

$N=5$		$h=0.05$			α
n	$\boldsymbol{i}_n$	η^j		MAD_n	α_n
1	(3,1,1,1,1)	$j=1$	2.10273E−3	3.95E−5	1
		$j=2$	2.16882E−3		
		$j=3$	2.20840E−3		
		$j=4$	2.24787E−3		
		$j=5$	2.31329E−3		
2	(1,3,1,1,1)	$j=1$	2.15632E−3	1.95E−5	2
		$j=2$	2.18889E−3		
		$j=3$	2.20840E−3		
		$j=4$	2.22788E−3		
		$j=5$	2.26025E−3		
3	(1,1,3,1,1)	$j=1$	2.20108E−3	2.74E−6	14
		$j=2$	2.20566E−3		
		$j=3$	2.20840E−3		
		$j=4$	2.21114E−3		
		$j=5$	2.21571E−3		
4	(1,1,1,3,1)	$j=1$	2.20733E−3	4.02E−7	98
		$j=2$	2.20800E−3		
		$j=3$	2.20840E−3		
		$j=4$	2.20881E−3		
		$j=5$	2.20948E−3		
5	(1,1,1,1,3)	$j=1$	2.20231E−3	2.28E−6	17
		$j=2$	2.20612E−3		
		$j=3$	2.20840E−3		
		$j=4$	2.21068E−3		
		$j=5$	2.21449E−3		

Table 7
Case 2: anisotropic grids for $2 \le q \le 7$.

q	2	3	4	5	6	7
Number of grids	4	6	9	12	16	20
Number of points	7	15	29	57	113	225

to 5×10^{-2}. The divergence free random velocity field is modeled by a Wiener process with covariance function

$$\mathbb{C}ov\left(t,t'\right) = \sigma^2 min\left\{t,t'\right\}, \tag{82}$$

where t, $t' \in [0,1]$. This process can be approximated by

$$w(\mathbf{Y},t) = \overline{\boldsymbol{w}} + \sigma \sum_{n=1}^{N} \sqrt{\lambda_n}\varphi_n(t)Y_n \tag{83}$$

where

$$\lambda_n = \frac{4}{\pi^2(2n-1)^2}; \quad \varphi_n(t) = \sqrt{2}sin\left(\frac{t}{\sqrt{\lambda_n}}\right), \quad n = 1,\ldots., \tag{84}$$

and $Y_n \in N(0,1), n = 1,\ldots,N$. Here we use $\overline{\boldsymbol{w}} = 1$ and $\sigma = 0.01$. Fig. 11 shows the covariance function, divided by σ^2, and the decay of the eigenvalues as n increases. The fast decay of the eigenvalues indicates that a good approximation for $w(\mathbf{Y},t)$ can be achieved with just a few terms of the KL expansion.

The postprocessing procedure used to identify the relative importance among the random directions is verified by using $N=3$ and $N=5$. For the last case, the stochastic grids $\boldsymbol{i}_n = (1,1,i_n,1,1)$ are constructed using either $i_n = 2$ or $i_n = 3$. Tables 4–6 present the estimate of the error with respect to the quantity of interest $\eta^j, 1 \le j \le 3,5$, for each stochastic grid. They also show the MAD_n for each case, as well as the resulting weight vector. Also in this case, we verified that either a higher N or higher level stochastic grid yield the same weight vector $\boldsymbol{\alpha}$, indicating that the proposed adaptive strategy is very robust to the initial choices for N, q and $\boldsymbol{i}_n$.

The weight vector $\boldsymbol{\alpha}$ is used to construct the anisotropic sparse grid by using Eq. (53). Table 7 indicates the number of partial grids used in the tensor product and the number of points of the final grid for $2 \le q \le 7$. For the anisotropic grid with $q=2$ we evaluate the estimate of the error in space with respect to the quantity of interest and perform the step (3) of the algorithm. Fig. 12 shows that estimate in space for all intermediate meshes. The convergence of the estimate of the variance of the error with respect to the quantity of interest is reached for $q=6$ and higher.

Using now the final spatial mesh and $q=6$, we increase N until the estimate of the variance of the error with respect to the quantity of interest becomes invariant, which happens for $N=4$. The mean and variance of the primal solution at $t=0.6$ obtained at the end of the algorithm are shown in Fig. 13. The variance exhibits a two symmetric

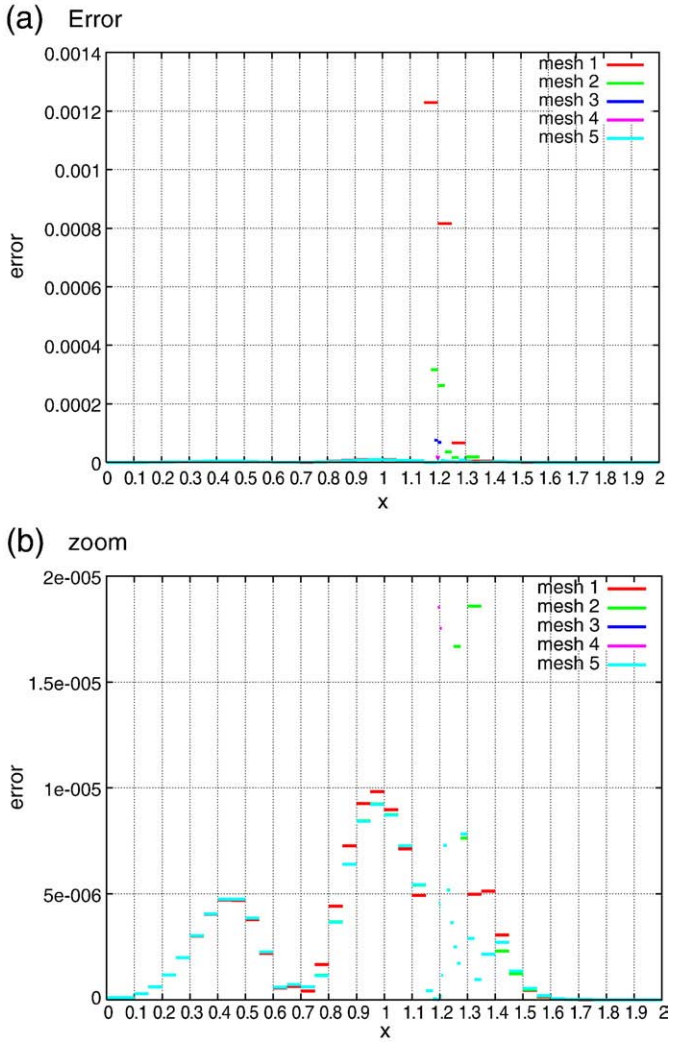

Fig. 12. Error η_{K_i} for all intermediate meshes.

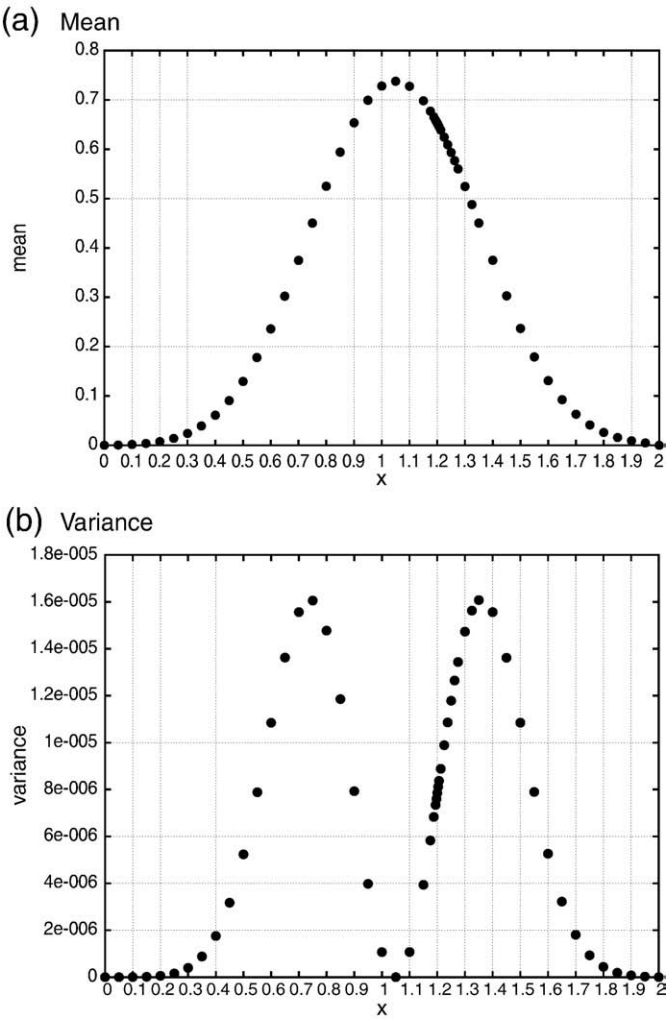

Fig. 13. Mean and variance of the primal solution at $t=0.6$.

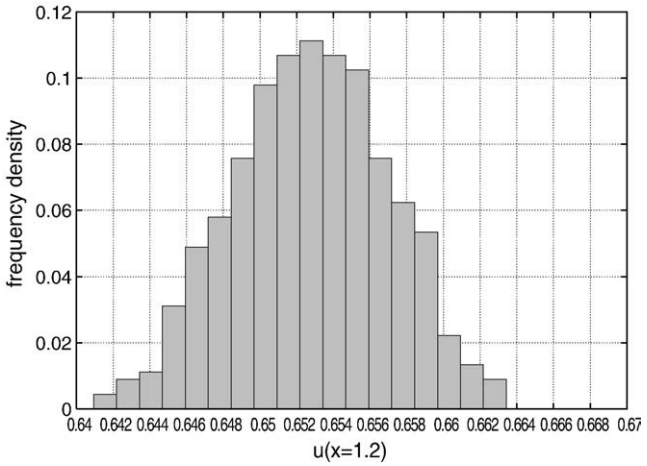

Fig. 14. Histogram of the primal solution at $x = 1.2$ and $t = 0.6$.

peak behavior around the center of the mean solution, where the variance is very small. Similar behavior is reported in [33]. The corresponding sample histogram of the primal solution at $x = 1.2$ is shown if Fig. 14 , which also has a normal distribution profile.

8. Conclusions

In this work we have described a general theory for goal-oriented error estimation for stochastic advection–diffusion models. The random parameters are approximated by Karhunen–Loève expansions and the non-intrusive stochastic collocation method is used for the numerical treatment of the resulting stochastic equations. This allows us to compute the error with respect to the selected quantity of interest by a series of deterministic primal and dual problems. The error estimates are used to guide an adaptive algorithm to adapt the physical mesh, the dimension of the random space and the collocation points. The dimension of the random space is chosen as small as possible to meet the prescribed accuracy with respect to the quantity of interest. The use of anisotropic tensor product grids in probabilistic space rather than isotropic sparse grids yields substantial savings for problems possessing natural anisotropy with respect to stochastic directions. The methodology has been successfully applied to a class of model problems in one space dimension.

Acknowledgments

This research is partially supported by the Brazilian Government, through the Agency CAPES (Coordenação de Aperfeiçoamento de Pessoal de Nível Superior), under grant # 0858/08-0. The first author also would like to acknowledge the support of the J.T. Oden Faculty Fellowship Research Program at ICES. The support of the work of JTO under DOE contract DE-FC52-08NA28615 in connection with the Predictive Science Academic Alliance Program is gratefully acknowledged. Additionally, support of JTO under research grant KAUST U.S. Limited: US 00003 is gratefully acknowledged.

References

[1] M. Ainsworth, J.T. Oden, A posteriori error estimation in finite element analysis, John Wiley & Sons, Inc., New York, 2000.
[2] S. Prudhomme, J.T. Oden, On goal-oriented error estimation for elliptic problems: application to the control of pointwise errors, Computer Methods in Applied Mechanics and Engineering 176 (1–4) (1999) 313–331, doi:10.1016/S0045-7825(98)00343-0.
[3] R. Becker, R. Rannacher, A feedback approach to a posteriori error control in finite element methods. basic analysis and examples, East–West Journal of Numerical Mathematics 4 (1996) 237.
[4] J. T. Oden, S. Prudhomme, Goal-oriented error estimation and adptivity for the finite element method, Tech. rep., TICAM Report, Austin (1999).
[5] J.T. Oden, K.S. Vemaganti, Estimation of local modeling error and goal-oriented adaptive modeling of heterogeneous materials: I. error estimates and adaptive algorithms, Journal of Computational Physics 164 (1) (2000) 22–47, doi:10.1006/jcph.2000.6585.
[6] J.T. Oden, T.I. Zohdi, Analysis and adaptive modeling of highly heterogeneous elastic structures, Computer Methods in Applied Mechanics and Engineering 148 (3–4) (1997) 367–391, doi:10.1016/S0045-7825(97)00032-7.
[7] K.S. Vemaganti, J.T. Oden, Estimation of local modeling error and goal-oriented adaptive modeling of heterogeneous materials: Part ii: a computational environment for adaptive modeling of heterogeneous elastic solids, Computer Methods in Applied Mechanics and Engineering 190 (46–47) (2001) 6089–6124, doi:10.1016/S0045-7825(01)00217-1.
[8] R.G. Ghanem, P.D. Spanos, Stochastic finite elements: a spectral approach, revised EditionDover Publications, Inc., New York, 2003.
[9] I. Babuška, R. Tempone, G.E. Zouraris, Galerkin finite element approximations for elliptic equations with random input data, SIAM Journal on Numerical Analysis 42 (2) (2004) 800–825.
[10] M. Bieri, C. Schwab, Sparse high order fem for elliptic spdes, Computer Methods in Applied Mechanics and Engineering 198 (13-14) (2009) 1149–1170, doi:10.1016/j.cma.2008.08.019 hOFEM07 - International Workshop on High-Order Finite Element Methods, 2007.
[11] M.K. Deb, I. Babuška, J.T. Oden, Solution of stochastic partial differential equations using galerkin finite element techniques, Computer Methods in Applied Mechanics and Engineering 190 (48) (2001) 6359–6372, doi:10.1016/S0045-7825(01)00237-7.
[12] C. Schwab, E. Süli, R.-A. Todor, Sparse finite element approximation of high-dimensional transport-dominated diffusion problems, ESAIM: Mathematical Modelling and Numerical Analysis 42 (2008) 777–819, doi:10.1051/m2an:2008027.
[13] I. Babuška, F. Nobile, R. Tempone, A stochastic collocation method for elliptic partial differential equations with random input data, SIAM Journal on Numerical Analysis 45 (3) (2007) 1005–1034, doi:10.1137/050645142.
[14] F. Nobile, R. Tempone, Analysis and implementation issues for the numerical approximation of parabolic equations with random coefficients, International Journal for Numerical Methods in Engineering 80 (6) (2009) 979–1006, doi:10.1002/nme.2656.
[15] F. Nobile, R. Tempone, C.G. Webster, An anisotropic sparse grid stochastic collocation method for partial differential equations with random input data, SIAM Journal on Numerical Analysis 46 (5) (2008) 2411–2442, doi:10.1137/070680540.
[16] D. Xiu, J.S. Hesthaven, High-order collocation methods for differential equations with random inputs, SIAM Journal on Scientific Computing 27 (3) (2005) 1118–1139, doi:10.1137/040615201.
[17] C. Schwab, R.-A. Todor, Karhunen-loeve approximation of random fields by generalized fast multipole methods, Journal of Computational Physics 217 (2006) 100–122, doi:10.1016/j.jcp. 2006.01.048.
[18] D. Xiu, Fast numerical methods for stochastic computations: a review, Communications in Computational Physics 5 (2–4) (2009) 242–272.
[19] F. Nobile, R. Tempone, C.G. Webster, A sparse grid stochastic collocation method for partial differential equations with random input data, SIAM Journal on Numerical Analysis 46 (5) (2008) 2309–2345, doi:10.1137/060663660.
[20] M.A. Tatang, W. Pan, R.G. Prinn, G.J. McRae, An efficient method for parametric uncertainty analysis of numerical geophysical models, Journal of Geophysical Research 102 (D18) (1997) 21,925–21,932.
[21] V. Barthelmann, E. Novak, K. Ritter, High dimensional polynomial interpolation on sparse grids, Advances in Computational Mathematics 12 (4) (2000) 273–288, doi:10.1023/A:1018977404843.
[22] H.-J. Bungartz, S. Dirnstorfer, Multivariate quadrature on adaptive sparse grids, Computing 71 (1) (2003) 89–114, doi:10.1007/s00607-003-0016-4.
[23] T. Gerstner, M. Griebel, Dimension adaptive tensor product quadrature, Computing 71 (1) (2003) 65–87, doi:10.1007/s00607-003-0015-5.
[24] B. Ganapathysubramaniana, N. Zabaras, Sparse grid collocation schemes for stochastic natural convection problems, Journal of Computational Physics 225 (1) (2007) 652–685, doi:10.1016/j.jcp. 2006.12.014.
[25] T. Gerstner, M. Griebel, Numerical integration using sparse grids, Numerical Algorithms 18 (1998) 209–232.
[26] C. Webster, Sparse collocation techniques for the numerical solution of stochastic partial differential equations with random input data, Ph.D. thesis, College of Arts and Sciences - The Florida State University, Tallahassee (2007).
[27] A.A. Oberai, J. Wanderer, A dynamic approach for evaluating parameters in a numerical method, International Journal for Numerical Methods in Engineering 62 (2005) 50–71, doi:10.1002/nme.1181.
[28] A.N. Brooks, T.J.R. Hughes, Streamline Upwind Petrov-Galerkin formulations for convection dominated flows with particular emphasis on the incompressible Navier-Stokes equations, Computer Methods in Applied Mechanics and Engineering 32 (1982) 199–259.
[29] J.T. Oden, S. Prudhomme, Error estimation and adptivity for the finite element method, Computers and Mathematics 41 (2001) 735–756.
[30] S. Prudhomme, J.T. Oden, Computable error estimators and adaptive techniques for fluid flow problems, Lecture Notes in Computational Science and Engineering, Error Estimation and Adaptive Discretization Methods in Computational Fluid Dynamics., 25, 2002, pp. 207–268.
[31] D. Xiu, S.J. Sherwin, Parametric uncertainty analysis of pulse wave propagation in a model of a human arterial network, Journal of Computational Physics 226 (2) (2007) 1385–1407, doi:10.1016/j.jcp. 2007.05.020.
[32] D. Xiu, J. Shen, Efficient stochastic galerkin methods for random diffusion equations, Journal of Computational Physics 228 (2) (2009) 266–281, doi:10.1016/j.jcp.2008.09.008.
[33] M. El-Amrani, M. Seaïd, A spectral stochastic semi-Lagrangian method for convection-diffusion equations with uncertainty, Journal of Scientific Computing 39 (3) (2009) 371–393, doi:10.1007/s10915-009-9273-5.